

**METEO
FRANCE**



RTP 10.10 / WW_MEDATLAS

Scientific Report

SLIE/IE Management reference :	Medatlas report 2003-4	Version :	1
Document reference :	RTP10.10/TR/IE's/04	Revision :	2
Date :	2004-04-14	Nb / pages :	75
		Nb/ appendices :	

	Function	Entity	Name	Date	Visa
Author :	IEPM	NTUA	G. ATHANASSOULIS Ch. STEFANAKOS	2004-04-14	
Author :	IEPM	ISMAR	L. CAVALERI	2004-04-14	
Author :	IEPM	Thetis	E. RAMIERI	2004-04-14	
Author :	IEPM	Semantic	C. NOËL	2004-04-14	
Author :	IEPM	Météo France	J.M. LEFEVRE	2004-04-14	
Approver :	PM	CS SI	P. GAILLARD	2004-04-14	

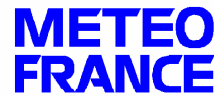
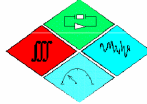
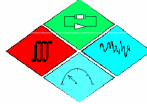


Table of Contents

1.	Foreword	1
1.1.	General Introduction	1
1.2.	Acknowledgements.....	3
2.	Introduction.....	4
2.1.	Aim of the project and of the atlas	4
2.2.	General description of the atlas content.....	4
2.3.	General outline of the applicability of the atlas.....	4
2.4.	Customers.....	6
2.4.1.	Western European Union – Research Cell.....	6
2.4.2.	Délégation Générale pour l’Armement (France).....	7
2.4.3.	The Ministry of Defence of the Republic of Italy	7
2.4.4.	Hellenic Ministry of National Defence / General Secretariat for Economic Planning and Defence Investments	7
2.5.	Partners	9
2.5.1.	CS	9
2.5.2.	NTUA.....	9
2.5.3.	ISMAR	10
2.5.4.	THETIS.....	11
2.5.5.	SEMANTIC TS.....	11
2.5.6.	METEO FRANCE	12
3.	Data sources	13
3.1.	Measured Data.....	14
3.1.1.	Buoy data	14
	Introduction.....	14
	The data	14
	Data errors	17
3.1.2.	Satellites data	17
	Introduction.....	17
	The data	17
	Calibration of the data	18
	Validation.....	18
	Data errors	20
3.2.	Model data	20
3.2.1.	The atmospheric model - wind data.....	22
3.2.2.	The WAM wave model	23
3.2.3.	The WAM model operational at ECMWF.....	24
3.2.4.	The results available at ECMWF	24
3.2.5.	Data errors.....	25



**METEO
FRANCE**

Scientific
Report
RTP10.10

3.3.	Data handling	26
4.	Calibration	27
4.1.	The data available for calibration	27
4.2.	Choice of points	27
4.3.	Calibration procedure	28
4.3.1.	Definition of calibration coefficients	28
4.3.2.	The combined use of the available data	29
4.3.3.	The calibration	32
4.4.	Analysis of the calibration procedure	33
5.	Statistical modelling and analysis of wind and waves	40
5.1.	Short term and long term statistical modelling of wind and waves	40
5.2.	Description of the data samples	44
5.3.	From original samples to grouped samples	46
5.3.1.	Criteria for data grouping	49
5.3.2.	Partitions of wind and wave parameters	50
5.3.3.	On the partition of the peak period T_p	50
5.4.	Analytic probability models	51
5.5.	Wind and wave climate in the Mediterranean Sea	54
5.5.1.	Wind statistics	55
5.5.2.	Wave statistics	59
5.5.3.	Joint statistics	63
6.	Reliability assessment of the atlas	64
6.1.	Critical analysis of the reliability of the calibrated data	64
6.2.	Geographical distribution of the reliability	65
7.	Printed Atlas	66
7.1.	Spatial distribution of statistical quantities	67
7.2.	Spatial distribution of probabilities of some important events	69
7.3.	Frequency tables of joint occurrences	70
8.	References	71

1. Foreword

1.1. General Introduction

It is obviously useful to have available a detailed and prolonged statistics of the wind and wave conditions in an area of interest. The WW-Medatlas project had the aim to produce such an atlas for the Mediterranean Sea, making use of the data and methodologies presently available.

Traditionally, extended wind and wave data in the open sea were available only from the visual reports by sailors. Notwithstanding the strong limitations, several atlases have been built from this source. The actual measurement of the wave conditions at specific locations became current practice with the introduction of the wave measuring buoys. Wind data in the open sea were more rare, as taken from special buoys or from open sea platforms. Then the satellite era began, with a steady flow of wind and wave data. At the same time the numerical models, both meteorological and wave ones, improved their accuracy to a point where their results could be reliably used for practical purposes.

This may look like an overwhelming amount of data. However, each source has its drawbacks and limitations. The buoys are very sparse, and only a limited number of them are available. Each satellite moves along a fix orbit, and the altimeter derived data are available only along its ground tracks, with large spaces between, at a time interval equal to the duration of the cycle, typically between 10 and 30 days. The numerical models are the densest source, both in space and time. However, they are models, and as such only an approximation to the truth.

The solution lies in the combined use of all these sources, complementing their various drawbacks with the data from an alternative source. This has been the principle followed for the preparation of this atlas.

Such a procedure is not straightforward and requires several steps. The data, both from the measurements and from the models, need to be collected, checked for possible macroscopic errors and eventually corrected. Then the various sources must be combined, providing the final dataset suitable for the final statistics. This report describes the overall procedure followed for the production of the atlas and the available results.

The present Atlas has been based on model data, appropriately calibrated by means of satellite altimeter measurements. In that way the systematic space-time coverage, a unique feature of numerical models, is fully exploited and, at the same time, the quality of the data and presented results is significantly improved by using the most up-to-date and reliable measurement technique able to cover large sea areas: satellite remote sensing.



**METEO
FRANCE**

Scientific
Report
RTP10.10

A 10-year data set consisting of 935 data points, distributed throughout the whole Mediterranean sea, has been collected, calibrated, analyzed and exploited in preparing the Atlas. Various important statistical parameters have been calculated for the main wind and wave characteristics, and their geographical distribution has been displayed, on a seasonal basis, by contour lines in 70 maps. Besides, 2580 bivariate histograms for the main wind and wave characteristics have been calculated (again on a seasonal basis) and presented for 129 points along the Mediterranean Sea, in the printed Atlas. All these results (maps, contour lines and histograms) are also available in electronic form, providing the user with additional, more flexible and more efficient, tools for treating and recovering the information he/she needs. In the electronic Atlas, histograms and related statistics are given for an extended set of 239 data points.

Neither measurements nor models are perfect. Therefore the user should not forget that the results here provided are only approximations of the truth. A detailed discussion of the accuracy of the results and of its geographical distribution is given in the text. However, we can confidently state that these are among the best data available in the Mediterranean Sea. A well thought use of the atlas would be the key to make the best of it.

1.2. Acknowledgements

The authors would like to thank :

- The Western European Union for their financial support,
- CNES (Centre National des Etudes Spatiales) and NASA (National Aeronautic and Space Agency) for having provided TOPEX altimeter data,
- ESA (European Space Agency) for having provided ERS altimeter data,
- the personnel of ECMWF for their help during the retrieval and the analysis of the wind and wave model data,
- Ente Publico Puertos del Estados, Clima Maritimo, Madrid, Spain,
- Ministry of Transport and Public Works, Sea Works Unit, Nicosia, Cyprus,
- National Center for Marine Research, Anavyssos, Greece, for providing with buoy data from their area of responsibility,
- Prof. I.V. Lavrenov, Arctic and Antarctic Research Institute, St. Petersburg, Russia, for a preliminary hindcast study of the Greek Seas

Among the many other people that we want to acknowledge for their contribution and support, we mention :

- Kostas Belibassakis, Yannis Georgiou, Panagiotis Gavriliadis and Yanna Rapti from NTUA for their support during the period 1999-2004
- A. Bergamasco who has contributed on Medatlas project as Thetis's project manager during the first 2 years,
- Nathalie Imperatrice, engineer at CS SI, for her contribution for producing the time series datasets of ten year length,
- Martine Pellen-Blin, Fabien Colombar, Philippe Cassou engineers at CS SI, for the ergonomic evaluation and software validation of the Electronic atlas and for quality control on deliverables.

2. Introduction

2.1. Aim of the project and of the atlas

This atlas is the result of the Medatlas project led between 1999 and 2004 by a consortia of six companies located in France, Italy and Greece (see section 2.5 for further information).

The main objective of this atlas is to provide reliable long term wind and waves statistics at specified points of the Mediterranean Sea at practically every offshore location (at about 50 km intervals).

2.2. General description of the atlas content

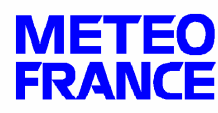
This atlas presents the results of the statistical analysis carried out on wind and wave data, spanning a ten year period collected and analysed by the participants.

These results are presented either in graphical form (charts) or in tabular form (bivariate histograms) which are described more in details in chapter 7.

2.3. General outline of the applicability of the atlas

The information contained in this Atlas can be used in various ways and for various different applications in Ship Design and Operational Planning, as well as in Offshore and Coastal Engineering. Among them, we mention, as examples, the following:

- **Operational Planning and Optimization of existing ships or fleet**
By defining margins of operationally acceptable environmental conditions for existing ships (single ship or a fleet), and using the information of the Atlas to assess probabilities, it is possible to calculate operability indices, optimize the overall efficiency of ships, reorganise the geographical distribution of a fleet etc.
- **Compare different designs by means of their operability indices**
- **Perform operational planning of offshore activities (naval or civil)**
 - Planning the seasonal window (e.g, month) of a war-at-sea exercise
 - Planning the seasonal window of a specific offshore activity (hauling up, dredging, construction)



- Planning the most appropriate period for organizing a sailing race
- **Ship Design**
For safety reasons, the key information is the extreme value of wind and wave parameters, which are not examined in this Atlas.
For assessing the operability of a specific design in a specific sea environment we have to study the efficiency/operability of this design in various sea states and the average by using the long-term probability of occurrence, which is provided by the Atlas.
- **Assess offshore wave energy resource**

2.4. Customers

2.4.1. Western European Union – Research Cell

"The current mission of the WEAO Research Cell is to provide the member nations of the WEAO with an efficient and effective service in the field of co-operative defence research and technology.

WHAT IS THE WEAO?

The Western European Armaments Organisation (WEAO) was created in Ostend in October 1996 by the adoption of its Charter and signature of the WEAO MOU by the then 13 members of WEAG. Its membership has since increased to 19. It is a subsidiary body of the WEU and shares in the WEU's legal personality. Although the WEAO Charter and MOU are the foundation documents for the creation of an European Armaments Agency, the Organisation is currently operating only as a Research Cell, known usually by the acronym WRC. Its offices are in Brussels, co-located with the WEU Secretariat and the Armaments Secretariat of WEAG. The Cell is headed by a General Manager, plus 13 members of staff, drawn from 8 different European countries. The General Manager is responsible to the Board of Directors of the WEAO; the Board is currently made up of the National Armaments Directors of the 19 member states, and meets in formal session in March and October each year.

WHAT DOES THE WRC DO?

The WRC provides the WEAO member states with a variety of services in the field of defence Research and Technology. Some are common services provided to all members, whilst some support specific groups of nations undertaking co-operative R&T projects.

The common services provided by the WRC include administrative support to the WEAO Board of Directors and the WEAG Panel II (the Research and Technology Panel of WEAG), and to their subsidiary groups and committees, and advice to WEAO members on a variety of matters to do with R&T co-operation. Collectively, the staff of the Cell have expertise in a wide variety of subjects; they include not only scientists, engineers and

contracts specialists, but also staff who are expert in IT, in MOU and general legal matters, in organisation and management of conferences, and of course in general administration in an international context. The WRC supports co-operative R&T projects by assisting the participating nations to prepare and sign the relevant project arrangements, by providing

administrative support to the project management teams when required, and by letting contracts for research work on behalf of the project participants. The Cell is able to let contracts using the legal personality of the WEU.

2.4.2. Délégation Générale pour l'Armement (France)

Established in April 1961 within the Ministry of Defence, the Délégation Générale pour l'Armement (DGA) prepares future defence capabilities and runs the development of materials as well as weapon systems to equip French Armed Forces.

DGA is in charge of designing and acquiring weapon systems to meet the needs expressed by Armed Forces. As such, it is tasked with preparing tomorrow's defence equipment and conducting armament programmes. DGA runs its activities in partnership with the headquarters staff, the users of equipment thus developed, and with armament industrialists who manufacture the equipment.

DGA's added value lies in its high level of technical skills as well as its ability to control risks involved in conducting particularly complex projects. DGA's position within the Ministry of Defence makes it a privileged representative able to provide an overall "joint-service" view. As a result, DGA has been offering France a chance to acquire high technology materials and weapons such as the Leclerc tank, the Charles-de-Gaulle Aircraft carrier and the Rafale aircraft.

2.4.3. The Ministry of Defence of the Republic of Italy

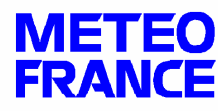
The Ministry of Defence of the Republic of Italy was officially established in May 1947, after the reunification of the earliest Ministries of the War, Navy and Air Force. The Minister of Defence is charged with implementation of security and defence guidelines established by the Government and approved by the Parliament. Being advised by the Chief of Defence Staff and the Secretary General of Defence/National Armaments Director, the Minister defines the guidelines related to military policy, intelligence and security, and technical/administrative activities.

The Secretary General of Defence/National Armaments Director is responsible for organization and management of technical, industrial and administrative Defence areas. He is also responsible for the activities of the Ministry of Defence related to research, development and procurement. Medatlas project (RTP10.10) has been managed and funded as part of these activities.

2.4.4. Hellenic Ministry of National Defence / General Secretariat for Economic Planning and Defence Investments

The Ministry of Defence (MoD) and the Hellenic Armed Forces under its command (Army, Navy, Air Force), implement the National Defence Policy decided upon by the Hellenic Government.

The Ministry of Defence focuses on issues related to defence policy, national defence design and planning, the structure of the Armed Forces, crisis management and the evaluation of intelligence material. In addition, relations with international organisations,



Scientific Report RTP10.10

personnel training and welfare, infrastructure and armaments, conscript recruitment policy, information technology and meteorology, as well as the social contribution of the Armed Forces, constitute major areas of MoD activity.

The General Secretariat for Economic Planning and Defence Investments is a separate body of the MOD, which supports the Minister in the areas of economic planning and budgeting, the implementation of armaments programs and expenditures, military compensatory benefits, the development of domestic defence industry and technology, and the optimal utilisation of the real estate portfolio of the National Defence Fund.

2.5. Partners

2.5.1. CS

CS (or CS SI) is positioned at the crossroads of information and communications systems, infrastructure installations and scientific and technical applications for both civilian and military use. Its comprehensive range of services includes systems design, integration and outsourcing. Nearly 70% of CS's work involves projects that span several years. CS builds long-term relationships with its customers and provides them with the solutions that are best suited to their needs and resources.

As MedAtlas Project SLIE (Single Legal Industrial Entity), CS has represented IEs (Industrial Entities) in front of Research and Technology Project (RTP) Research Cell (RC) and Management Group (MG). As such, CS was responsible for the overall project management and holds the interface to the MG for all administrative and technical aspects of the MEDATLAS project. Responsible for carrying out the MedAtlas project in good conditions and as official interlocutor of the MG for the contract execution, CS has been specially in charge of :

- Contract management, and technical control for the Work Packages (WPs),
- MG consultation for every request of the project evolution,
- Co-ordination in Consortium,
- In collaboration with each IE, technical progresses assessment of each WP and reporting towards the MG,
- Meetings preparation and leading.

In addition, CS has taken part in:

- Data base creation, loading and administration,
- Ergonomic evaluation and software validation of the Electronic atlas,
- Data migration in order to provide not calibrated data in time series format for all the 935 points and ten years period.

2.5.2. NTUA

NATIONAL TECHNICAL UNIVERSITY of ATHENS (NTUA) is the oldest technical university in Greece, covering all disciplines of engineering. The University is divided into nine academic departments and operates about a hundred laboratories within the sphere of its technological competence.

The School of Naval Architecture and Marine Engineering, which is one of the most active departments at NTUA, consists of four Divisions and operates four Laboratories. In the Division of Ship and Marine Hydrodynamics, the Sea Wave Research Group is being

involved, through academic research and European and National projects, in research concerning wave modelling and wave transformation, wave-body interaction problems, coastal hydrodynamics, ocean wave statistics, stochastic modelling of wave climate, wave energy, remote sensing, marine geographical information systems, integrated graphical user interfaces for marine/coastal applications, and marine atlases both in electronic and paper form.

The main contributions of NTUA in the present project are:

- the systematic derivation of long-term wind and wave statistics, including empirical probability densities and the appropriate probabilistic modelling of the various parameters studied (univariate, bivariate, directional, time series),
- the systematic production of charts and tables for the various wind & wave parameters, and
- the design, realisation and publication of the Printed form of the atlas, including the design of the cover page.

Apart from the above major contributions, NTUA has also contributed to :

- the collection of in situ measurements,
- the development of the user-interface,
- the design and development of graphical presentation software,
- the testing and validation of the Electronic version of the atlas.

2.5.3. ISMAR

One of the largest institutes of CNR, the Italian National Research Council, ISMAR (formerly ISDGM) has three main lines of activity, devoted respectively to the study of coastal areas and lagoons, geology and oceanography. Within the last section, numerical modelling has a prominent role, focused on circulation and wave modelling, in both deep and shallow water. While ISMAR has no operational role, the institute has contributed to the development and implementation of many operational models in Italy and abroad.

Given its previous experience, the main role of ISMAR in this project was the partly retrieval, the handling and calibration of the ECMWF wind and wave data. Ten years of data have been screened and homogenised to take into account the changes occurred in the models during the whole period. The data, available as fields, have been transformed into time series at each of the points chosen for late consideration in the atlas.

The satellite data provided by Meteo France have been prepared for comparison with model data. The distribution of co-located values have been carefully analysed with sophisticated statistical tools deriving correction coefficients for both wind and wave model parameters at each chosen location. These coefficients have been analysed for consistency and used to obtain the final calibrated model results.

ISMAR has done a critical analysis of the errors present in the model and satellite data, and derived an estimate of the accuracy of the calibrated data and of its geographical distribution. It has provided the wave data for the Italian network, to be used for the

assessment of the quality of the altimeter data. It has also used these data for an assessment of the performance of the ECMWF wind and wave models in the Mediterranean Sea. ISMAR has carried out statistics for the wind and wave model data, estimating in particular the dominant wind and wave directions at the single grid points and the spatial variability of the overall fields.

2.5.4. THETIS

Thetis is a Technological Centre based in the historic Arsenale of Venice. Thetis operates as a systems integrator in the development of projects, services and innovative technological applications in two business areas:

- Environmental and civil engineering:
- System analysis; specialist and environmental impact studies; environmental monitoring systems and services; environmental informatics; dissemination of technical and scientific information.
- Facility management; restoration and rehabilitation of historic buildings; technologies for urban maintenance; structural integrity monitoring systems; project management.
- Intelligent Transport Systems (ITS)
- GPS localisation and fleet management systems and services for public transport applications; maritime and inland navigation management systems (VTMIS, Vessel Traffic Management Information Services).

The main contribution of Thetis in MedAtlas project was to develop the electronic version of the Mediterranean wind and wave atlas. This activity initially concentrated on the conceptual design of the electronic application and the definition of its general architecture. Afterward Thetis developed the electronic atlas interface and produced different application releases. These were evaluated by customers and partners, as well as subjected to specific ergonomic analyses and validation plans.

Finally, Thetis integrated data (bivariate frequency tables, spatial distribution of statistical quantities, spatial distribution of probabilities of important events) in the electronic atlas and performed an accurate final evaluation.

The software MapObject version LT of the ESRI family was used to develop the electronic atlas.

2.5.5. SEMANTIC TS

SEMANTIC-TS is a French SME specialized in research and development, from development of physical idea and its mathematical modelling, to implementation of in situ measurement or signal processing system. Semantic TS company conducts studies, develops specific softwares, and organizes measurement campaigns in the areas of oceanography, time-frequency domain, underwater acoustics, environment and signal processing.

Contribution of SEMANTIC TS remains first in calculating directional statistics of wave data

and building a tool for NTUA's analyses of the data. WAM hindast wave data have been made available and processed and directional statistics have been calculated (polar histogram and wave rose). Results have been presented in a web site which constitutes a useful tool because it gathers, in a unique site, observable in any computer environment, all the available information which was in different formats. This allowed facilities to analyze data and synthesize results.

On a second hand, SEMANTIC TS has used available buoys and altimeters wave data in the Mediterranean Sea for a validation and calibration of altimeter data. Data from 15 Mediterranean buoys and from Topex and ERS satellites have been collected and processed, in order to create collocation files and show comparison statistics. Collocation results web sites have been computed as well as a sensibility study, and analysed in collaboration with METEO FRANCE.

2.5.6. METEO FRANCE

Météo-France, a public administration placed under the authority of the Ministry of Transport and Housing, is the French organisation responsible for supplying information nationwide on the state of the atmosphere, of the ocean upper layer and the repercussions this may have on human life and property. Meteo-France is also a member state of the European Centre for Medium-Range Weather Forecasting (ECMWF). Among the necessary activities to meet these requirements, Météo-France, receives, processes and archives information supplied by observing systems, among them one finds polar orbiting environment satellites. Météo-France also analyses all this information and feeds it into numerical prediction models, either at global scale or over areas of particular interest.

As a meteorological service, the main contribution of Météo-France in this project was to collect data from numerical weather prediction models, from numerical wave prediction models and from satellite altimeters and scatterometers, for a ten years period for the whole Mediterranean sea.

Then, because of its experience in using satellite data for improving and validating wave model analyses, Meteo-France was in charge of the validation/calibration of the satellite data that have been used to correct the model data. Among the wave models in the Mediterranean sea, the most extended source is provided by ECMWF. The ERS near real time data (Fast Delivery Products) from the European Space Agency (ESA) have been archived at Météo-France. The TOPEX/Poseidon Geophysical Data Records (GDR's) have been provided by CNES, the French space agency. Once validated and calibrated using results from global studies, the altimeters wave data have been validated for the Mediterranean Sea using buoys data collected for the project, in collaboration with SEMANTIC TS.

3. Data sources

There are four main sources of marine wind and wave data available to the user:

- visual observations from ships,
- data measured from buoys or platforms,
- data measured by remote instruments on board of high altitude flying satellites,
- meteorological and wave models operational at the various meteo-oceanographic centres.

These data have different characteristics expressed as quality, accuracy, errors present in the data, geographical distributions, number of data. In the following sections we give a brief description of the data and of their use when assembling the atlas. In particular we list also the problems and consequent limitations associated to each source and instrument.

Remark about visual estimates :

Taken from ships of opportunity, this has been for a long time the only source of information for wind and wave data in the open sea. Many decades of data exist, and a full generation of atlases has been based on these data. However, careful comparisons with properly measured data have shown the limitations of this approach and the substantial errors potentially present in the reported data, particularly in stormy conditions, the situation that users care more about. From the point of view of the atlas of a full basin, a major limitation of the visual data is given by their preferential distribution along the most common maritime routes, and by the tendency of the ships to avoid the stormy areas, in so doing substantially biasing the statistics that can be derived.

Given the large availability of alternative data, that, combined in an optimal way (see later sections), provide a good accuracy and a complete coverage in space and time, no use has been made of visual estimates in the preparation of this atlas.

3.1. Measured Data

3.1.1. Buoy data

Introduction

This has become since a while ago the standard method for the collection of wave data in the open sea. The data are measured from a floating buoy, moored at a given location. The local depth can reach a few hundreds metres, with the exclusion of very shallow water (a few metres).

The data

The most common supplier of this kind of buoys has been Datawell, from Netherlands. The first buoy was the Waverider, a surface following sphere including a stabilised vertical accelerometer. The related signal is transmitted to land on a continuous basis, where it is recorded at predetermined intervals. The limit of this buoy is its capability of measuring only the vertical component of motion of the surface. Hence no directional information is available.

The Waverider was followed by the Wavec, a much larger version with the capability of recording also directional information. Also this buoy is based on the principle of surface following. Therefore measuring the motion of the buoy corresponds to know how the local geometrical characteristics of the sea surface change with time. The physical quantities measured are the surface elevation and the two orthogonal components of the surface slope. Proper mathematical handling of these quantities provides estimate of the elevation frequency spectrum, and of the dependence on frequency of mean wave direction, skewness and kurtosis. Further integration leads to the integral parameters significant wave height H_s , mean direction q_m , peak and mean period T_p and T_m .

The Wavec buoy is quite large, its overall diameter, once assembled, measuring more than 3 metres. The weight is more than 700 kg. While this poses obvious difficulties for its handling, it is also a deterrent to the improper removal or damaging of the buoy. As the Waverider, the Wavec buoy is characterised by a very high reliability. During more than ten years of operation in the network around Italy (RON, De Boni et al., 1993) the data obtained amount to more than 90% of the theoretical maximum. The interruptions have been due mainly to software problems in the transmission of the data from the land station to the central collection office.

As the Waverider, the Wavec buoy is continuously in operation, i.e. the signal carrying the measurements is continuously transmitted. The sequence of recording is purely a strategic decision, based on a trade-off between the information made available, the amount of repetitive information and the associated volume of storage. In general a three-hour interval is chosen between two sequential records, to be taken at synoptic times (00, 03, 06, ... UT), to be eventually reduced in case of a severe storm. In more recent times the Wavec has been progressively substituted by the Directional Waverider, a much lighter version still with directional capabilities.

A substantial number of these buoys, either Waverider or Wavec or Directional Waverider, are distributed along the coasts of the Mediterranean Sea. A summary of the situation, including the satellite data discussed in the next section, is given in Table 1. The Table provides the location, its geographical coordinates, the local depth, and the period for which the data were available for this project. The most substantial source of buoy data was given by the Italian network RON (De Boni et al., 1993). However, a large network exists also along the Spanish coastline. Table 2 lists the information available from the single sources.

Table 1 - Sum-up of buoys and satellite information

Physical source	Geographical zone	Site	File header code	Program code	Beginning of campaign	End	Latitude (deg)	Longitude (deg)	Depth (m)
Buoy	Spain	Cabo de Palos	0	CAB	14/11/85	16/11/98	37°65. N	0°64. W	67
		Mahon	1	MAH	29/04/93	01/01/95	39°72. N	4°44. E	300
		Palamos	2	PAL	25/04/88	21/09/98	41°83. N	3°19. E	90
	Cyprus	Cape Arnaoutis	3	ARN	26/03/93	04/02/98	35°9.16' N	32°15.88' E	
	Northern Crete	1	4	CR1	01/02/94	30/11/94	35°22.31' N	24°27.58' E	10
		2	5	CR2			35°22.65' N	24°27.57' E	20
		3	6	CR3			35°24.55' N	24°27.22' E	100
	Italian coasts	La Spezia	7	SPE	01/07/89	31/12/98	43°55.7 N	09°49.6 E	80
		Pescara	8	PES			42°28.2 N	14°28.2 E	80
		Monopoli	9	MON			40°58.5 N	17°22.6 E	80
		Crotone	10	CRO			39°01.4 N	17°13.2 E	80
		Catania	11	CAT			37°26.4 N	15°08.8 E	80
		Mazara del Vallo	12	MAZ			37°31.5 N	12°32.0 E	80
		Ponza	13	PON			40°52.0 N	12°57.0 E	100
Alghero	14	ALG	40°32.9 N	08°06.4 E	80				
Satellite	Mediterranean Sea	Topex	15	TOP	01/08/91	30/06/02			
		ERS 1-2	16	ERS					

Table 2 - Kind of data provided by each file

Physical source	Geographical zone	Site	Date							Hs	/q	Tp	Tz	Tm	S(fp)	Wind speed
			Year	Month	Day	Hour	Min	Sec								
Buoy	Spain	Cabo de Palos	*	*	*	*			*			*				
		Mahon	*	*	*	*			*	*		*				
		Palamos	*	*	*	*			*			*				
	Cyprus	Cape Arnaoutis	*	*	*	*			*	*	*	*				
	Northern Crete	1														
		2	*	*	*	*	*			*	*	*	*		*	
		3														
	Italian coasts	La Spezia														
		Pescara														
		Monopoli														
Crotone		*	*	*	*	*			*	*	*		*			
Catania																
Mazara del Vallo																
Ponza																
Alghero																
Satellite	Mediterranean Sea	Topex ERS 1-2	*	*	*	*	*	*	*						*	

For the purposes of this atlas the data are available as the four integral parameters mentioned above, i.e.:

H_s significant wave height (metres),

q_m direction (degrees, clockwise with respect to geographic North),

T_p peak period (seconds),

T_m mean period (seconds).

However abundant, it is obvious from Table 1 and Table 2 that the buoy data are far from being sufficient for characterising completely the climate of the Mediterranean Sea. As it will be clear from the final data, this sea shows very strong spatial gradients in the values of wave height, period and direction, basically a consequence of its complicated geometry and its subdivision in different sub-basins. Besides the buoys are mostly located very close to the coasts, in so doing being hardly representative of the conditions in the open sea. A major limitation, at least for the buoys used in the Mediterranean Sea, is the lack of wind data.

Data errors

In the Mediterranean Sea the buoys represent the most accurate source of information for wave data. The error is estimated in the order of few percents. The error grows substantially when we move to the highest wave heights, for the tendency of the buoys to slip around the highest crests, in so doing underestimating the overall wave height.

3.1.2. Satellites data

Introduction

Satellite radar altimeters provide an estimate of the significant wave height along the off nadir satellite track by measuring the slope of the return pulse leading edge, which is stretched out in time because of the delay between reflections from the wave crests and the wave troughs. They also provide an estimate of the wind speed (at ten meter above sea level) by measuring the radar cross section, which is a function of the small scale roughness of the sea surface. Scatterometers provide an estimate of the 10m wind vectors on the 500 km width swath by measuring the radar cross section at different incident angles. The data from three satellites were used to calibrate the model data: ERS1, ERS2 and TOPEX/Poseidon. The ERS near real time data (Fast Delivery Products) from the European Space Agency (ESA) have been archived at Météo-France. The TOPEX/Poseidon Geophysical Data Records (GDR) have been provided by CNES, the French space agency.

The data

Wave height and wind speed from ERS1, ERS2 altimeters (from 08/1991 to 06/2002), TOPEX altimeter (from 01/1993 to 06/2002) and wind vectors from ERS1 and ERS2 scatterometers (from 08/1991 to 06/2002) have been extracted from the METEO-FRANCE archive in BUFR code and from the AVISO Altimetry data based in VAX/VMS format.

The ERS1 and ERS2 data are the FDP (Fast Delivery Products) distributed on the GTS (Global Transmitting System).

Between 11/04/96 and 01/06/1996 both satellites ERS1 and ERS2 have been disseminated data in quasi real time. Before 11/04/96 only ERS1 have been are distributed as FDP and after 01/06/1996, only ERS2 data have been distributed.

The data have been converted in Ascii for a selected area (covering the Mediterranean Sea). A quality control procedure has been applied to the data. Some spurious data have been eliminated : several flags or index have been tested in order to eliminate most of the spurious data. The data have been finally calibrated. The significant wave height and the wind speed from ERS1, ERS2, TOPEX_A and TOPEX_B altimeters have been corrected according to relations deduced from comparisons with buoys measurements, cross comparisons between altimeters, and global analyses of the evolution of the significant wave height (SWH).

Calibration of the data

1/ Topex data

The significant wave height and the wind speed from TOPEX altimeter have been corrected according to relations deduced from comparisons with buoys measurements (Cotton et al, 1997, Lefèvre and Cotton 2001).

$$SWH_{cor.} = 1.052 SWH_{gdr} - 0.094$$

$$U10_{cor.} = 0.87 U10_{gdr} + 0.68$$

For TOPEX data, linear time dependant correction has been applied to the Ku band data in order to correct a maximum bias of 40 cm for cycle 236 (31/01/1999), starting from no correction at cycle 132.

2/ ERS altimeter data

The following regression relation, from Queffeulou (1994), has been used to correct the FDP swh for ERS1:

$$SWH_{cor.} = 1.32 * SWH_{fdp} - 0.72$$

For the ERS-2 FDP swh, the following regression relation from Queffeulou (1996) has been applied:

$$SWH_{cor.} = 1.09 SWH_{fdp} - 0.12$$

Validation

Once the satellite data were calibrated using results from global studies, a further validation of altimeter data in the Mediterranean Sea has been done using the locally available buoys and altimeters wave data. The aim was to compare data from buoys and satellites. As there is no data about wind speed from buoys, only Hs has been compared. To make the comparison possible, a collocation procedure (time and space) is needed. Obviously this can be done only with a certain approximation. The closer they are, the most significant is the comparison. The comparison can be done with different approximations in time (T) and space (D), and for different ranges of wave height (H). Then T, D and H can be considered as parameters.

Data from 15 Mediterranean buoys and from Topex and ERS satellites have been collected and processed. Tools adapted to collocation files creation and analysis have been first developed. That means:

- a database containing all the data
- a tool able to realise collocation on buoys and satellite data : that means to enhance comparable data with different set of the parameters T, D and H

- a tool able, after each collocation configuration, to
 - calculate statistics over the data gathered :

Num	Number of values	N
Xm	Mean of HsB	$\frac{1}{N} \sum_{i=1}^N HsB_i$
Var X	Variance of HsB	$\frac{1}{N} \sum_{i=1}^N (HsB_i - HsBm)^2$
Ym	Mean of HsS	$\frac{1}{N} \sum_{i=1}^N HsS_i$
Var Y	Variance of HsS	$\frac{1}{N} \sum_{i=1}^N (HsS_i - HsSm)^2$
Slop	Symmetric slope	$\frac{\sum_{i=1}^N HsB_i HsS_i}{\sum_{i=1}^N HsB_i^2}$

- build a web site containing all the data, the statistical and graphical results computed.

Validations of the tool have been performed and collocation results web sites have been computed as well as a sensitivity one. Figure 1 shows an example of scatter diagram obtained for Alghero buoy and Topex_A data, in a distance of 40 km and 2 h; the number of collocated values is 96. Satellite and buoy data are rather coherent.

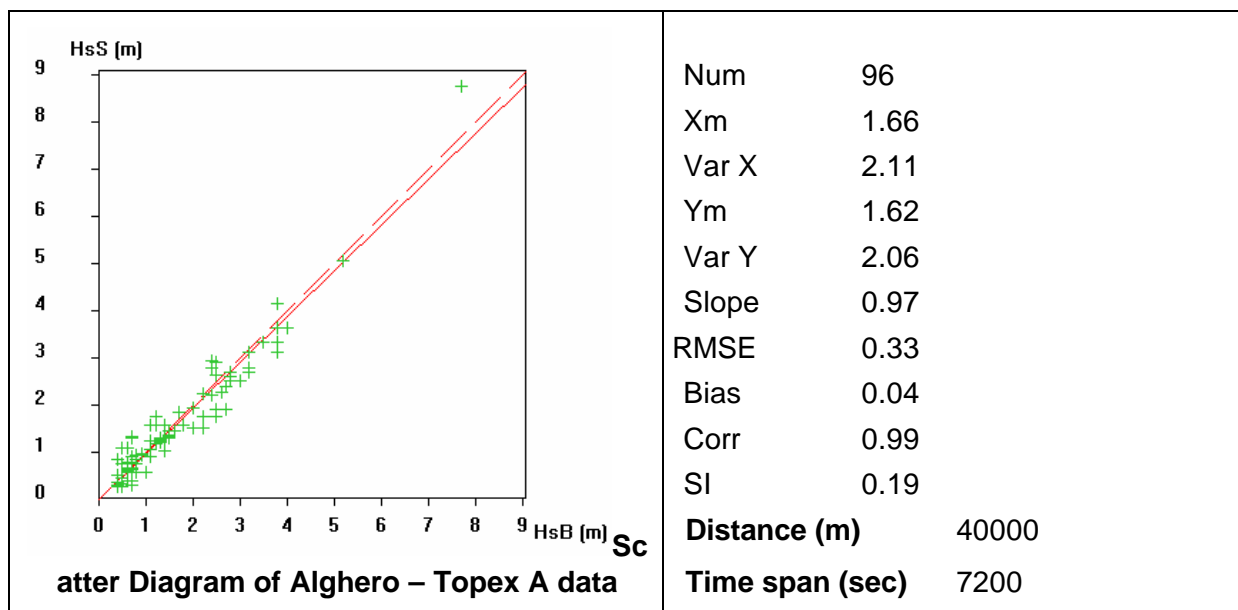


Figure 1 - Scatter diagram and related statistics between Topex_A and buoy wave heights at Alghero (Sardinia, Italy).

The analysis of all these results has been made through systematic comparisons between buoys data and altimeters. The main conclusion was that we did not notice any need for an additional calibration of the satellite data.

Data errors

Due to the tracking of the signal, data from off-shore tracks are not flagged as valid typically within the first 20 km. Also, because of the contamination of the signal by land echo and of the size of the radar altimeter footprint, data from on-shore tracks are not flagged as valid within typically the first 5 km.

The scatterometer is also not able to estimate the wind vector close to the coast (typically at the location of the most coastal sea point of the wave model).

For waves below 1 m, the error on the altimeter significant wave height is quite big (more than 0.5 m) and waves below 0.5 m are set to a value close to 0.5 m, generating a wrong distribution of the wave height around 0.5 m. The problem for low waves has been mentioned for ERS FDP's data by Challenor and Cotton (1997). Also, the linear correction used is not valid for waves below 1 m for ERS2 altimeter. On Table 3 below, the specified accuracy for each instrument is given together with the achieved accuracy, from Cotton and al. (1997) for the altimeters and from the ERS ESA user handbook for the scatterometer.

Table 3 - Specified and achieved accuracy of satellite instruments

Satellite/Instrument		Specified range	Specified accuracy	Achieved accuracy
ERS1-2 Altimeter FDP	Wave height	0-20 m	0.5 m or 10%	0.3 m
	Wind Speed	0-24 m/s	2 m/s	1.5m/s
TOPEX/Poseidon Altimeter GDR	Wave Height	0-20 m	0.5 m or 10%	0.3 m
	Wind Speed	0-24 m/s	2 m/s	1.5 m/s
ERS1-2 Scatterometer FDP	Wind Speed	1-28 m/s	2 m/s or 10%	

3.2. Model data

Many different institutions run global atmospheric and wave models, producing daily forecast and analysis worldwide. However in general, these models, and in particular the wave ones, do not have a resolution high enough to describe with sufficient accuracy the fields in the inner basins, like the Mediterranean Sea. For this reasons, some of these institutions, who have a particular interest in this basin and/or in the surrounding areas, run locally a limited area version of their models.

Indeed, it turns out that several sources of information are presently available for the

Mediterranean Sea. The list includes the U.K. Meteorological Office (UKMO), the European Centre for Medium-Range Weather Forecasts (ECMWF, Reading, U.K.), Meteo France, and the U.S. Navy Oceanographic Center. However, once we start specifying the conditions for the data required for long term statistics, the list shrinks considerably. The conditions we ask for are:

- availability of data for at least a decade on the whole Mediterranean basin, with an accuracy and resolution compatible with the project,
- free availability of data, or at least at a cost compatible with the budget of the project.

The first condition limits the choice to ECMWF and UKMO. The meteorological and wave models used at UKMO and ECMWF are rather different. ECMWF run a global meteorological model, with a resolution that has been gradually increasing in time. The wave model is Wam, an advanced third generation model based on first physical principles and briefly described later in this section. A complete description of the model is found in Komen et al (1994). Practically since the start of its operation, two versions of Wam have been run, one for the globe, and another one with a higher resolution for the Mediterranean Sea, lately extended to the whole North Atlantic area. Traditionally UKMO have run two versions of their meteorological model, one for the globe, and another, with a higher resolution, nested in the previous one, for the European area. Parallel to this, two versions of their wave model were used, again with different resolutions. Regarding the wave model, UKMO is still running an old second generation wave model, that has been repeatedly reported to show problems with the advection of swell. This is connected to another characteristic of the UKMO wave model, i.e. the limited number of frequencies used to resolve the wave spectrum. In connection with the aims of WW-Medatlas, this is particularly negative as it implies a crude approximation to the determination of the peak frequency, a key information for the atlas and for navigation.

ISMAR (formerly ISDGM) has made use for a long time of both the sources, and extensive intercomparisons have been done, see, e.g. Cavaleri et al (1991), and Dell'Osso et al (1992). A basic problem with the UKMO limited area atmospheric model (LAM) was that the lower border of their LAM grid was at 30 degree North latitude, that corresponds to the most southern border of the Mediterranean Sea (Sirte gulf). This reflected the focus of interest of UKMO on the British Isles. The problem lies in the boundary conditions at the outer border of a LAM grid. At this position they are coincident with the local ones from the global model. A LAM shows its power (more defined details of the fields, typically higher wind speeds, etc.) in the inner part of its grid. Therefore, while the UKMO LAM achieved its aim on UK, it was not so effective on the Mediterranean Sea, particularly in its most southern part.

In the long term, but in any case within the first part of the last decade, the ISMAR experience has been that, notwithstanding the different resolutions, the quality of the products from the two centres was comparable, with possibly a better capability by ECMWF to carve out details of the fields. After this period a direct comparison in the Mediterranean Sea has not been a straightforward matter, due to the heavy commercialisation put on by UKMO. Using a three-year long intercomparison among different wind and wave models Bidlot et al. (2001) found the following results between UKMO and ECMWF:

- the results for wind speed are quite similar,
- UKMO has a slightly smaller bias for wave height, but with a larger scatter,
- UKMO has by far the worst results for T_p , because of the smaller number of frequencies

considered.

On top of this, UKMO make available their products for a fee much higher than the one requested by ECMWF. All the above conditions have led to the final choice of ECMWF as official source for the data to be used for the atlas. In the following paragraphs we give a brief description of the models used at the Centre and of the available results.

3.2.1. The atmospheric model - wind data

The operational model at ECMWF is spectral, i.e. the horizontal fields are described by a two-dimensional expansion of spherical harmonics truncated at, e.g., 319 (T319). The truncation identifies the resolution, here defined as half the smallest resolved wave length, used to describe the fields. For T319 it is $40,000/(2 \times 319) \cong 63$ km. Advection is calculated with a semi-Lagrangian scheme, while the physics is carried out on a reduced Gaussian grid in physical space. The vertical structure of the atmosphere is described by a multi-level hybrid σ coordinate system. The physical parameterisations describe the basic physical processes connected to radiative transfer, turbulent mixing, subgrid-scale orographic drag, moist convection, clouds and surface soil processes. The prognostic variables include wind components, temperature, specific humidity, liquid/ice water content and cloud fraction. Parameterisation schemes are necessary in order to properly describe the impact of subgrid-scale mechanisms on the large scale flow of the atmosphere. Forecast weather parameters, such as the two-metre temperature, precipitation and cloud cover, are computed by the physical parameterisation of the model. The ten metre wind is derived with a boundary layer model from the lowest σ level, 0.997, corresponding to about 30 metre height. A compact description of the model can be found in Simmons (1991) and Simmons et al (1995).

The horizontal resolution and the number of levels with which the atmosphere is described in the model has varied in time. T213 (95 km resolution) and 31 levels were used from 1991 till 1998, when ECMWF passed to T319. This change had a limited effect, because the Gaussian grid, used to model the processes in physical space, was not changed. The big step ahead came in November 2000, when the Centre passed to T511 (about 40 km resolution), with 60 levels on the vertical and a 40 km resolution Gaussian grid. Cavaleri and Bertotti (2003a) have clearly shown how a different resolution implies a different quality of the results. In the Mediterranean Sea this corresponded to an appreciable increase of the wind speeds, a fact to be considered in the evaluation of the calibrated data and of the final statistics.

Errors – The model data at very low wind speeds are not reliable because the situation is dominated by sub-grid processes. This is particularly true close to land, an obvious example being the land-sea breezes.

In the coastal areas the model winds are unreliable in all the conditions because of the dominant influence of orography, not properly represented in the meteorological model because of limited resolution (95 km for T213, 40 km for T511). Also the limited accuracy with which the actual coastline is represented into the model introduces errors in the coastal wind fields.

In offshore blowing conditions the winds are strongly underestimated, much more than off the coast. This problem is not yet completely understood, but dominant roles are likely to be

played by the orography and by the modelling of the marine boundary layer (see Cavaleri and Bertotti, 2003b).

There is a tendency to underestimate the peak wind speeds more than the average and low ones. This is probably connected to the resolution of the model, but the proper parameterisation of the physical processes active in heavy storm conditions is likely to play a role.

3.2.2. The WAM wave model

Since July 1992 the European Centre for Medium-Range Weather Forecasts run, parallel to their meteorological model, a wave model. Similarly to the weather forecast, the aim is to produce a forecast of the wave conditions.

The wave model used at ECMWF is WAM, an advanced third generation model developed with the co-operative effort of most of the experts available at the time. The two master references are WAM-DI (1988) and Komen et al (1994). Only a brief description, sufficient for the purposes of the report, is given here. The interested reader is referred to the above references for a full description and explanation.

The model stands on the spectral description of the sea surface, i.e. at all the points of the grid covering the area of interest the wave conditions are represented as the superposition of a finite, but large, number of sinusoidal components, each characterised by frequency f (Hz), direction \mathbf{q}_m (flow, degrees cwrgn), and height h (metres), hence energy F , proportional to h^2 . The evolution in time and space of the whole field is governed by the so-called energy balance equation

$$\frac{\partial F}{\partial t} + c_g \cdot \nabla F = S_{in} + S_{nl} + S_{dis} \quad (1)$$

where the left-hand terms represent the time derivative and the kinematics of the field, and the right-hand ones the physical processes at work for its evolution. More specifically:

- $\partial/\partial t$ is the derivative with respect to time,
- c_g is the group speed,
- $\tilde{\nabla}F$ represents the spatial gradient in the field.

Given the area covered by the model, the input information is provided by the driving wind fields, i.e. at each point by the modulus and direction of U10 (wind speed). More specifically, U10 is used, together with the wave conditions existing at that time at that point, to evaluate the friction velocity, hence the surface stress that expresses the actual transfer of momentum from wind to waves.

The term S_{dis} summarises the energy loss by the various dissipation processes at work. For all practical terms the only dissipative term of significance in deep-water is white-capping, i.e. the breaking that appears at the crest of the waves under the action of wind. More processes appear when the waves enter a shallow water area, the two most prominent ones being bottom friction and depth induced breaking. It is worthwhile to point out that the shallow water area is the least accurate part of the model. Together with other factors

discussed later, this hampers the use of model data in the very shallow coastal zones. However, this is not relevant for the present project, that, because of its purposes, is going to focus its attention mainly in the deep water zone.

The fourth-order nonlinear wave-wave interactions S_{nl} represent the conservative exchange of energy between the different wave components that takes place continuously during the evolution of the field.

All the above processes are correctly represented in the WAM model via their proper equations. The model is numerically integrated through a semi-implicit scheme, while advection is done with a first order upwind scheme. Because of requirements for numerical stability, the integration time step depends on the grid resolution, being 20 minutes for 0.5 degree, 15 minutes for 0.25 degree resolution.

3.2.3. The WAM model operational at ECMWF

Two versions of the WAM model have been operational at ECMWF, one for the global ocean and one for the Mediterranean Sea. The reason for doing this is the maximum resolution allowed for the global version because of computer power limitations, and the contemporary requirements to go to a higher resolution to properly describe the geometrical characteristics of the Mediterranean basin.

The wave model for the Mediterranean Sea became operational in July 1992. A 0.5 degree resolution was used in both latitude and longitude, for an overall number of about 950 points (WAM considers only sea points in its description of the basin). The resolution was later increased to 0.25 degree, for an overall almost 4000 points.

The original wave model for the Mediterranean Sea included the area between 6° West and 36° East in longitude, and 30° and 46° North in latitude. The area was later extended to include the Baltic Sea. In the Fall of 1998 a much more extended version was made operative. It includes the North Atlantic Ocean, the Barents Sea, the Baltic Sea, the Mediterranean Sea, and the Black Sea. The resolution is still 0.25 degree, but only in the latitude direction. For each latitude a different number of points has been used in the longitude direction, uniformly distributed at 27.5 km distance, more exactly at a distance corresponding to 0.25 degree in the latitude direction. This implies that the grid points are staggered and some further manipulation is required during the advection phase.

The number of frequencies has been kept constant at $N_f=25$, with $f_1=0.04$ Hz and $f_{n+1}=1.1 \cdot f_n$. $N_d=12$ directions have been used for most of the time, increased to 24 in correspondence of the expansion of the interested area in the Fall of 1998.

3.2.4. The results available at ECMWF

The information available at any moment of the integration process is represented, at any grid point, by the energy available for each wave component, i.e. by the two-dimensional spectrum $F(f, \mathbf{q})$. From this spectrum a number of quantities is evaluated.

An integration on directions provides the one-dimensional spectrum $E(f)$, i.e. a description of the energy distribution with frequency. A further integration on frequency provides the

overall energy E , from which the significant wave height H_s is derived. Different integrations provide estimates of the mean period T_m , sometimes called energy period, and the mean direction q_m . The formulas for the different parameters are given below.

$$E(f) = \int F(f, \mathbf{q}) d\mathbf{q} \quad (2)$$

The n -th order moments of the frequency spectrum are defined as

$$m_n = \int E(f) f^n df \quad (3)$$

from which

$$H_s = 4\sqrt{m_0} \quad (4)$$

$$T_m = \frac{m_{-1}}{m_0} \quad (5)$$

$$q_m = \tan^{-1} \frac{\iint F(f, \mathbf{q}) \sin q df d\mathbf{q}}{\iint F(f, \mathbf{q}) \cos q df d\mathbf{q}} \quad (6)$$

Note that in practical applications the integrals are substituted by finite summations.

The integral wave parameters available from the ECMWF archive have been retrieved for the Mediterranean area starting from 1 July 1992. The fields are available at 00, 06, 12, 18 UT of each day. The data have been taken with 0.5 degree resolution between the geographical limits present in the first version of the model at ECMWF, i.e. between 6° West and 36° East for longitude, and 30° and 46° North for latitude. This corresponds to a 85x33 point grid, out of which about 950 are sea points. Values on land are given as -1.0, an impossible value for any wave parameter.

3.2.5. Data errors

The model wave data are not reliable at combined low wave heights and periods because associated to light winds. Given (see above) that these are not reliable, a similar uncertainty follows also for the corresponding wave heights.

The model has a tendency to miss the peaks of a storm more than the general tendency to underestimate the wave heights in the Mediterranean Sea (connection with the underestimate of the wind speeds, see above).

The wave data have a lower reliability close to the coasts in case of inshore blowing winds because of the already mentioned poor accuracy of winds in these conditions. If the wind is blowing offshore the wave data can be substantially wrong till at least 50, most likely 100, km from the coast, because of the errors in the driving wind field (see above) and the approximation in the definition of the coastline due to the resolution of the wave model grid. The latter point is even more true during the first years considered for this analysis because

of the 0.5 degree (55km) resolution used at the time.

The integration algorithm used in the WAM model led to an underestimate of the wave heights in the early stages of wave generation, typically in the first 100-200 km off the coasts in offshore blowing wind conditions. This algorithm was corrected in December 1996.

For a few years all the model wave data in the low height range have strongly been biased towards upper values. The reason was a bug into the altimeter software of ERS2 that provided minimum wave heights of 1-1.2 metre also for much lower wave heights. These data were assimilated into the operational analysis, i.e. the data used for this atlas. Therefore the low height model data are strongly biased towards larger values.

Three different grids were used during the decade considered for the present analysis. Originally at 0.5 degree resolution, both in latitude and longitude, after a few years the model grid was upgraded to 0.25 degree, to be then changed again to a staggered one with 27.5 km resolution (regular in latitude, irregular in longitude). The associated approximation on the definition of the coastline has made some grid points to be land on one grid and sea in another one, and vice versa.

3.3. Data handling

From what we have said in the previous sections we conclude that:

- the buoy data are very accurate, but far from enough in space to suffice for the proper description of the characteristics of the whole Mediterranean Sea,
- the satellite data have a good quality, with the exception of very low and very large wind and wave values, and of the areas close to the coasts, especially when the satellite is flying toward offshore. There is a very large number of data available. However, for a specific location the data exists only at large time intervals (10 or 30 days depending on the satellite, more frequent for scatterometer wind). For the altimeter, the only source for wave height data, these are available only along the ground tracks of the satellite orbits,
- the model data are continuous in space and time, hence ideal for the purpose of the atlas. However, both the wind and wave data show a marked tendency to underestimate the corresponding measured values. Independently on this, the data are unreliable for low and very large values and in general close to the coasts, till a distance of 50-100 km.

It is clear that no single source suffices for providing suitable data for the atlas. The solution lies in the combined use of all the sources, reaching the best available results. The buoys are used to validate the satellite data. Then the latter ones are used to calibrate the wind and wave model results. Finally the calibrated data are used to derive the statistics for all the chosen points. The various stages of this procedure is the subject of the following chapter.

4. Calibration

In this chapter we summarise the data potentially available for calibration, the choice of the usable ones depending on a number of conditions, the procedure followed for the calibration and the problems connected with the input data and consequently the results.

The model parameters calibrated on the base of the satellite data are:

- wind speed
- wave height
- wave period

Only the first two parameters were actually derived from satellite measurements. The calibration of the wave period has been derived from that for wave height. No correction of direction has been introduced. Wherever checks were possible, we found that the direction was well estimated by the models, at least for non negligible values of the parameters.

4.1. The data available for calibration

As specified in the previous chapter, we have available different data-sets from different satellite instruments, for both wind speed and wave height. Specifically we have:

- wave height : Topex altimeter ERS1-2 altimeter
- wind speed : Topex altimeter ERS1-2 altimeter ERS1-2 scatterometer

These will be used to calibrate the model wind and wave data from the ECMWF archive. These data are available, with some limitations, for the decade from July 1992 till June 2002.

4.2. Choice of points

To keep the volume of the atlas within reasonable limits, we have considered a reduced number of points with respect to the more than 900 with 0.5 degree resolution used for retrieving the data from the ECMWF archive. Besides, in some part of the Mediterranean Sea, typically the more open basins, the spatial gradients of the wind and wave characteristics are likely to be more limited than in the smaller basins enclosed by coasts.

Two choices have been made. For the electronic version of the atlas we have chosen 239 points. Most of these are at one degree interval both in latitude and longitude,

complemented by some sparse points in the most critical areas, namely the Ligurian Sea, the Adriatic Sea, and the Aegean Sea. For the printed version the number has been reduced to 129, a subset of the larger choice, obtained selecting one point out of two in each direction, with staggered selection on adjacent lines, again complemented with extra points in the mentioned areas.

4.3. Calibration procedure

4.3.1. Definition of calibration coefficients

For each data-set and for each single satellite measurement, e.g. the ECMWF and the Topex measured wind speeds, the model data have been interpolated in space and time at the satellite position and time of passes. Then, each couple of data (model value and satellite measurement) has been assigned to the closest grid sea point. Parallel to that of the retrieved model data, this has taken place at 0.5 degree resolution. This has provided for each grid point a sequence of couples of data, sparse in time, suitable for a local analysis. For each point the model-sat distribution has been approximated with a best-fit straight line, passing through the origin. An example is given in Figure 2. The slope of the fit provides an estimate of the average ratio between model and satellite data, hence the inverse of the calibration factor to be used (corrected model = model * calibration factor *ca*).

Following what said in the previous chapter, the Topex *ca* values are available only at a limited number of positions, more or less along the Topex tracks. For each data-set, only points with a number of data larger than 200 have been considered. It was found that a smaller number was leading to occasional local *ca* values clearly off the physical range.

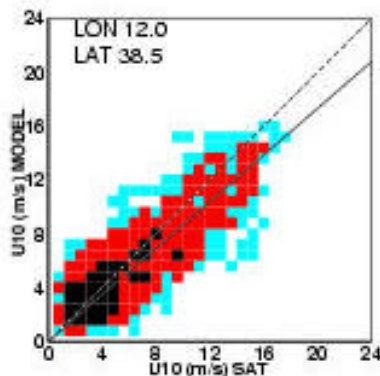


Figure 2 – Scatter diagram between model (vertical) and altimeter (horizontal) wind speeds at one grid point in the Mediterranean Sea.

The best-fit line is forced to pass through the origin. The scatter around it provides an indication of the reliability of the derived calibration coefficient

Even if the Topex data, hence the best-fit values A , are available only at part of the points in the Mediterranean Sea (the ones along the ground track of the satellite), to get a general idea of their characteristics we have plotted in Figure 3 the distribution of A for wind speed. Note that the values of A have been multiplied by 100, so that 100 represent in the figures a perfect fit between model and satellite data. By looking at the figure, we recognize at once the substantial underestimate by the model, particularly in the northern parts of the basin. More specifically, strong underestimates, for both wind and waves, are found in the areas with the more complicated geometry, and possibly with a complicated orography in the nearby land. It is easy to identify specific problems in the northern part of the Tyrrhenian Sea, in the Adriatic Sea and in the Aegean Sea.

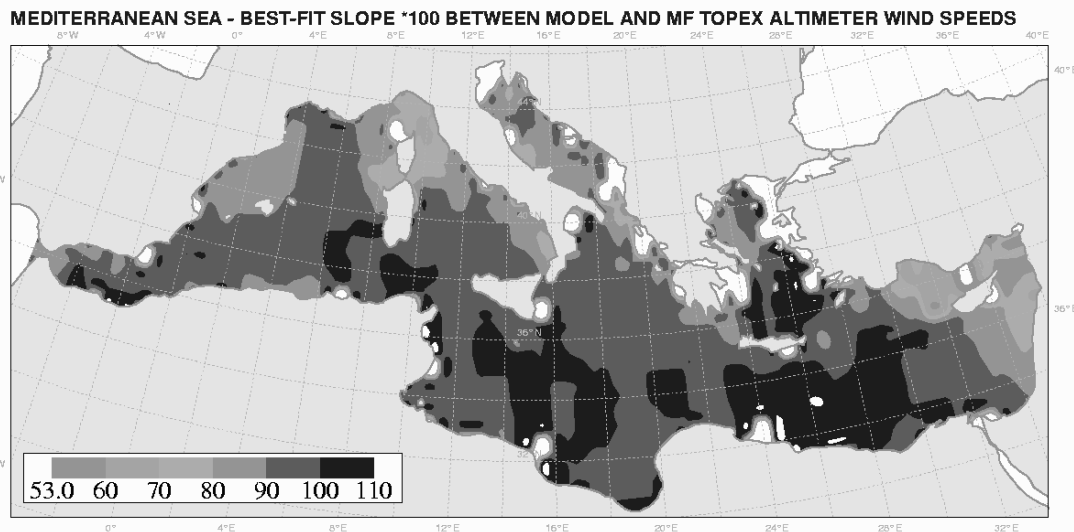


Figure 3 – Distribution of the slope of the best-fit lines between model and Topex altimeter wind speed values at the various grid points in the Mediterranean Sea. The single values have been multiplied by 100.

The above results are summarised in Figure 4, where we have plotted the statistical distributions of the best-fit slope values, for both wind speed and wave height. There is an evident average underestimate of both wind speeds U and wave heights H_s by the models. The values for U are peaked almost on the unity (unity represents a perfect model on the average), with a long tail towards lower values. Values as low as 0.5 are found. The values for wave height are much lower. No value is larger than one, all being lower than 0.90, with a peak at about 0.75, and values as low as 0.4. These very low values are typically found in the three areas mentioned above.

4.3.2. The combined use of the available data

Having different instruments measuring the same parameter at, in general, different times, we can expect, on the base of both statistics and the characteristics of the instruments, to find different calibration factors at the same location. For wave height, following the superior quality of the Topex data, one could think to use these data for the final calibration. However, the Topex *cal* values are not available at all the grid points we are interested in,

because of the sparse distribution of the tracks. On the other hand ERS1-2 provides an almost complete geographical coverage for *cal*. After a careful analysis of the data, it has been decided to use both the sources, weighting them according to their different reliability. The coefficients used for the overall calibration are :

wave height :	Topex altimeter	ERS1-2 altimeter
	0.65	0.35

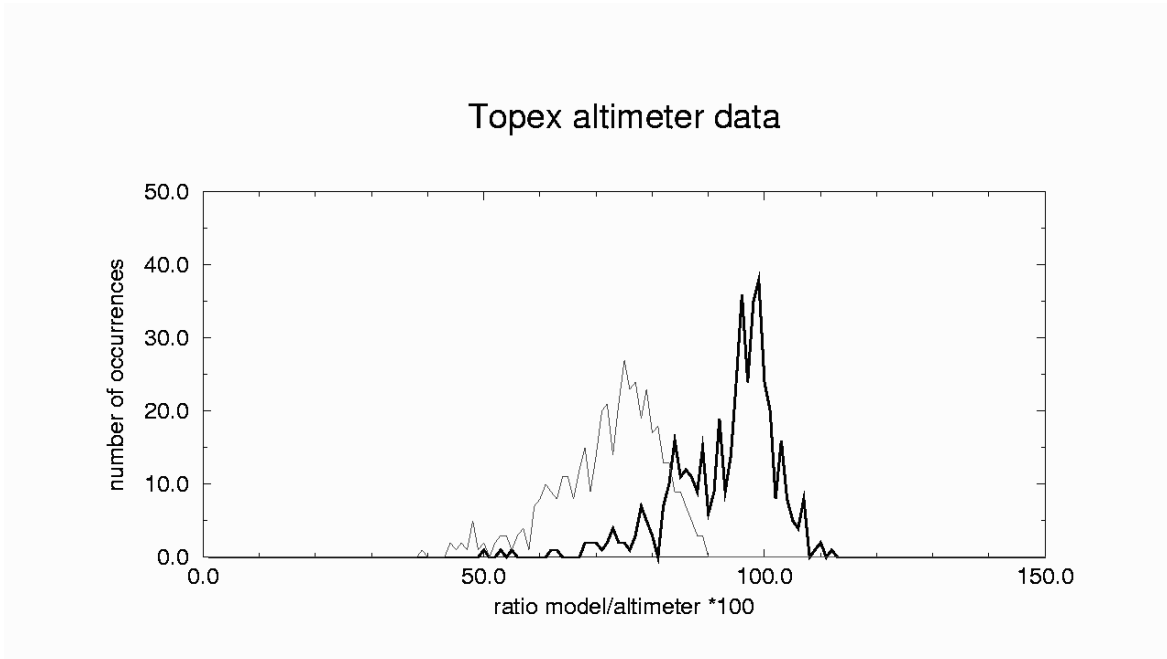


Figure 4 – Statistical distributions of the best-fit slopes between model and Topex altimeter data in the Mediterranean Sea.

The thick line refers to wind speed, the thin one to wave height. The slope values have been multiplied by 100.

At the points where no Topex data are available, the above technique implies that the ERS1-2 results are automatically accepted. However, a direct inspection of the the best-fit slopes of the wave height model data against the ones from Topex and ERS1-2 shows the Topex slopes to be lower by 3%. Figure 5 shows, separately for wind speed and wave height, the scatter diagrams between the model/sat best-fit values obtained using ERS1-2 and Topex at the grid points where the latter data are available. Therefore the ERS1-2 derived values have been multiplied by 0.97 to obtain values consistent with the ones derived from Topex.

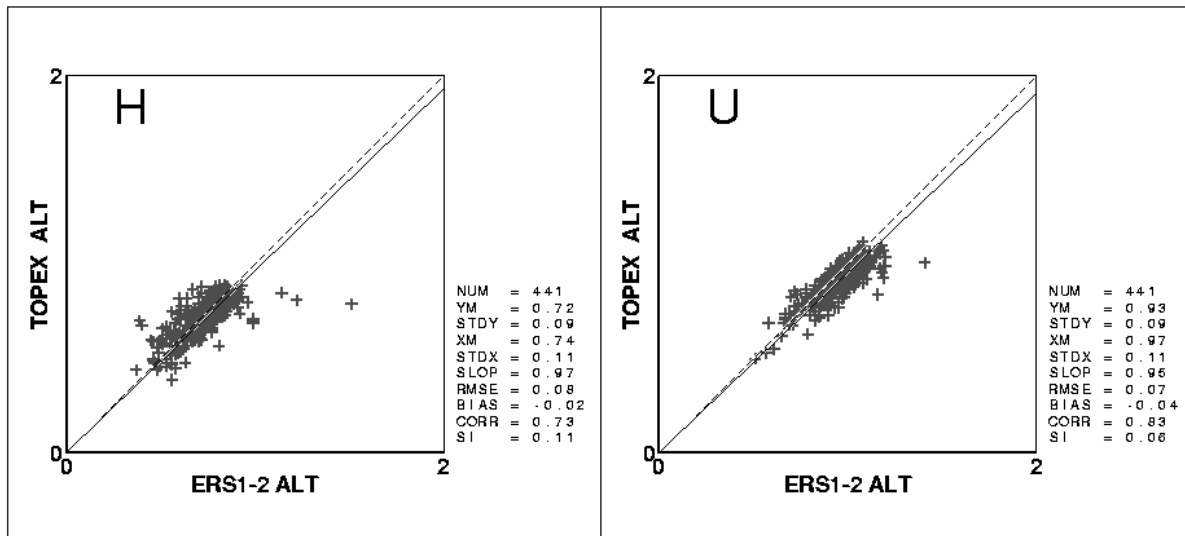


Figure 5 – Comparison between the “model vs satellite” best-fit slopes derived from ERS1-2 and Topex altimeter data.

The left diagram refers to wave height, the right one to wind speed

For wind speed a similar analysis has shown the ERS1-2 altimeter derived slopes to be lower by 4-5% with respect to Topex and by 2% with respect to the scatterometer. For the wind speed an analysis of the quality of data from the different sources would suggest as weighting coefficients:

wind speed :	Topex altimeter	ERS1-2 altimeter	ERS1-2 scatterometer
	0.35	0.25	0.40

The most complete source for wind would be the scatterometer, with the advantage of providing along its swath a two dimensional view of the fields. While not essential for calibration, this can be useful to give a better idea of the behaviour of the model. However, for our present interests there is a fundamental problem with these data. The meteorological models rely heavily on measured data made available in almost real time to produce the best analysis, before starting with the new forecast. This is done with data assimilation, i.e. correcting the model estimates on the basis of the measured data. The scatterometers have been, and still are, one of the main sources of information for the meteorological models.

The correction done with data assimilation does not affect the whole field of wind speed at the same extent. It is relevant in the area of the measurements, gradually fading when moving away from it. This implies that the resulting modelled wind fields do not have the same accuracy at all the locations. It is higher at the point where and when measured data have been available, lower otherwise. This is already a source of variability in the quality of the data. However, the crucial point is that, when we compare modelled and scatterometer wind speeds, this happens to be exactly at the locations where the model had already been corrected. In other words, the comparison is biased, and it does not represent the actual quality of the general model data. It follows that we cannot use the scatterometer data for a long term correction of the wind data set we have at disposal. Indeed, this information is still extremely useful in studying the general fields, but it is not so for our present purpose of a

general calibration.

The same is true for the ERS1-2 altimeter data. Two different data sets are available from the ERS1-2 satellites: the fast delivery products and the controlled ones, made available after a considerable time. The former ones are available in almost real time (within a few hours), and they are the ones used for data assimilation. These are also the ones used for the WW-Medatlas project.

The ERS2 altimeter wave heights have been assimilated into the WAM wave model at ECMWF since 1998. Therefore, as for the scatterometer, we cannot use these data for the calibration in the Mediterranean Sea after this date..

The ERS2 wave height data have another problem. There has been a permanent malfunctioning of the altimeter, when measuring the wave heights. Whichever the sea state, the reported measured data are almost always above 1-1.2 metre. Therefore the low wave height data are biased towards higher values. At ECMWF this was realised after some years, with a consequent bias of the ECMWF analysis data available from the archive. Because the H_s correction done when assimilating the ERS2 altimeter data was reflected also in the correction of the period, this is biased as well.

Summarising, the situation is the following:

- the scatterometer data cannot be used for calibration,
- the ERS2 wave height data cannot be used for calibration after 1998,
- we know that the analysis data used for the atlas are biased towards higher values in the low H_s range.
- Therefore for the actual calibration we can make use of the following data:
- wind speed, Topex and ERS1-2 altimeter data,
- wave height, Topex altimeter data; ERS-1 altimeter data, i.e. till 1995; ERS-2 altimeter data, only for sufficiently large wave heights, and only till 1998.

The weighting coefficients are the ones or proportional to the ones indicated above, till the case of unity when a single instrument was available.

4.3.3. The calibration

Following the procedure outlined above, the single calibration coefficients for wind speed (*calu*) and wave height (*calh*) have been derived at the various grid points. Because the geographical distributions of *calu* and *calh* show an unrealistic variability, the overall information has been summarised in the calibration coefficients only at the selected points, whose values has been derived with a careful analysis of the values at the surrounding not-considered-for-atlas grid points.

After extracting from the model data the time series, at 6-hour interval, at all the grid points, they have been calibrated by multiplying the single parameters by the proper calibration factor. As derived from previous experiences (Barstow et al, 2001, pp.17-18), an underestimate of H_s does not change appreciably the average wave steepness. Therefore the wave length changes proportionally to H_s . Given that the wave length varies, at least in

deep water, with the square of the wave period (deep water are assumed throughout the Mediterranean Sea), the periods are to be corrected multiplying them by \sqrt{calh} . No correction is introduced in direction, as it has long been recognised that the meteorological model provides a very good description of the overall pattern, hence directions are maintained. Therefore the final time series have been obtained multiplying the above quantities by:

- H_s $calh$
- DirH no correction
- T_p \sqrt{calh}
- T_m \sqrt{calh}
- U $calu$
- DirU no correction

This procedure has been applied separately to the data before and after 20 November 2000, i.e. when the substantial change of resolution in the operational ECMWF meteorological model implied a change of quality of the wind, hence wave, fields. Therefore for the first period we have at disposal 101 months of data, and only 19 for the later one.

4.4. Analysis of the calibration procedure

In this section we analyse the accuracy of the calibrated data, wind speed and wave height, in the Mediterranean Sea.

In a previous chapter we have pointed out that there is a number of random errors in the calibration. They mainly concern the measurements by the satellites and the capability by the models to respond to different situations. These errors lead to the large scatter we find in the best-fit at each specific location. This is also the reason why we find an unrealistic spatial variability of the calibration coefficients, that forces to summarise the information only at the selected points. Each selected point represents the summary of the information available in the surrounding area. This variability is present also in the open sea, where there is no physical reason for it. It shows the lack of reliability of the single estimates of the best-fit slopes. However, the variability increases even more when we move close to the coasts, particularly along the northern coasts of the Mediterranean Sea. The reason is that the whole European coast is characterised by a marked orography. As most of the storms that affect the Mediterranean Sea come from the northern sectors, the marine areas along the northern coasts are on the lee of the mountains. We have already mentioned that the altimeter data of wind speed are not accurate up to the specifications in the first 100 km off the coast. Assimilated in the meteorological model, their error is transmitted also to the wave field.

We can have an idea of the consequent uncertainty of the final estimate of the calibration coefficients by considering the scatter index SI of the single best-fits. SI is defined as the ratio between the root mean square (rms) error σ (model – measured datum) and the average value of the interested quantity, either wind speed U or significant wave height H_s . In practice SI provides a non-dimensional estimate of σ . The distributions of the SI values

in the Mediterranean Sea, for U and H_s , are given in Figure 6 and Figure 7, respectively. This information is an essential complement of the data provided by the atlas, to be presented with all the statistics there included.

We have to consider also the systematic errors. They are hidden, because in general they do not appear in the best-fit procedure. They do so when the errors have been corrected at a certain date. This is the case with the results of the WAM model in the first 100-200 km off the coast. In this range the previous integration scheme was biased towards low values. As already discussed in a previous chapter, this was corrected in the operational model in December 1996. Therefore before this date all the short fetch data have a permanent error towards the low values. Given the directions most of the storms come from, this is particularly true along the northern coasts of the Mediterranean Sea.

In principle the systematic errors are taken into account with the calibration. However, this is not always true for two reasons. In the specific example the bias is more marked in the low wave height range (early stages of generation off the coasts). When fitting a best-fit line to the data, the slope depends on the whole set, and therefore only a partial correction to the low range data is introduced, disrupting at the same time the fit to the larger values. This is reflected also in the variability of the ratio model/measurements. This is also the case for the continuous upgradings of both the meteorological and wave models at ECMWF. We can take into account the most substantial changes, as done for the passage to T511 in November 2000. However, it is not possible to split the calibration into a number of small periods, because the resulting reliability would be too low. Indeed this is partially the case for the period November 2000 – June 2002. With only 19 months at disposal, and a substantial decrease of the percentage of data available from the satellites, the results for this period have a lower reliability than for 1992 – 2000.

Looking at the results of the calibration, we find some inconsistency between the wind and wave results. The waves are a direct product of the wind, and any error in the generating wind field is reflected in the resulting wave field. Therefore the two maps of the calibration coefficients are expected to show a high degree of consistency. Indeed, this is the case for their geometrical distributions in the Mediterranean Sea, shown in Figure 8 for the wind speed and Figure 9 for the wave height. For both wind and waves, higher corrections are required along the European coasts and Turkey. However, the actual figures are not fully consistent. The corrections for wind are much lower than what one could guess using the ones for waves. In other words, the calibrated wind speeds are too low with respect to the calibrated wave heights. Indeed, this could be due to an error in the wave model, that could underestimate the wave heights. However, it is amply accepted in the literature (see Komen et al, 1994, Janssen, 1998, Swail and Cox, 2000) that the error of a sophisticated wave model, as it is the case with WAM, is substantially lower than those of the generating wind fields. As a matter of fact, the distribution of the wave heights in a basin, compared to the locally available measurements, is one of the best ways to judge the quality of the input wind fields. Therefore the inconsistency we have noted, of the order of at least 5%, is not expected to be a product of the wave model.

Our overall conclusions on the calibration are the following.

We believe we have obtained what can be considered as the best dataset of wind and wave data presently available in the Mediterranean Sea. However, some characteristics and limitations of the data should be kept in mind.

For both wind and waves the slope of the best-fit lines grows markedly moving southwards, across the basin. The largest errors are found along the northern coasts, larger where the smaller basins are characterised by a marked orography.

The accuracy of the best-fit slopes, hence of the calibration coefficients, can be derived from the scatter of the data around the best-fit lines. Maps have been provided showing the distribution of the scatter index (a non-dimensional measure of the rms error) in the basin for both wind speed and wave height.

The data in the lower range of wave heights are less reliable than the other ones. This is due to an error in the wave model before a certain date and to a problem with the corresponding measurements by the ERS2 altimeter.

The calibration coefficients for wind and waves are not fully consistent to each other. The calibrated wind speeds are low by at least 5% with respect to the calibrated wave heights.

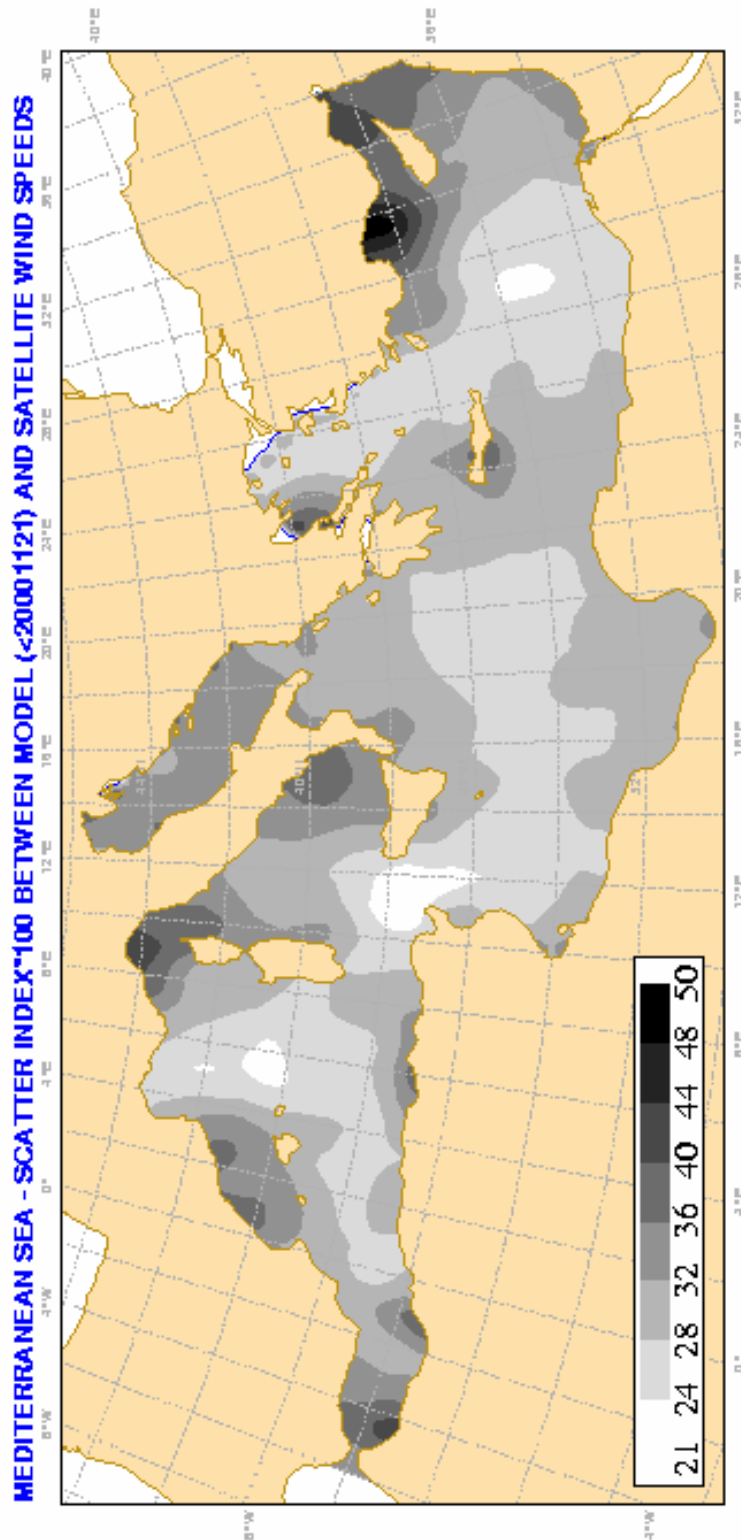


Figure 6 – Distribution of the scatter index of the best-fit between modelled and satellite measured wind speeds.
 Figures are in percent. The period considered is before 21_November 2000.

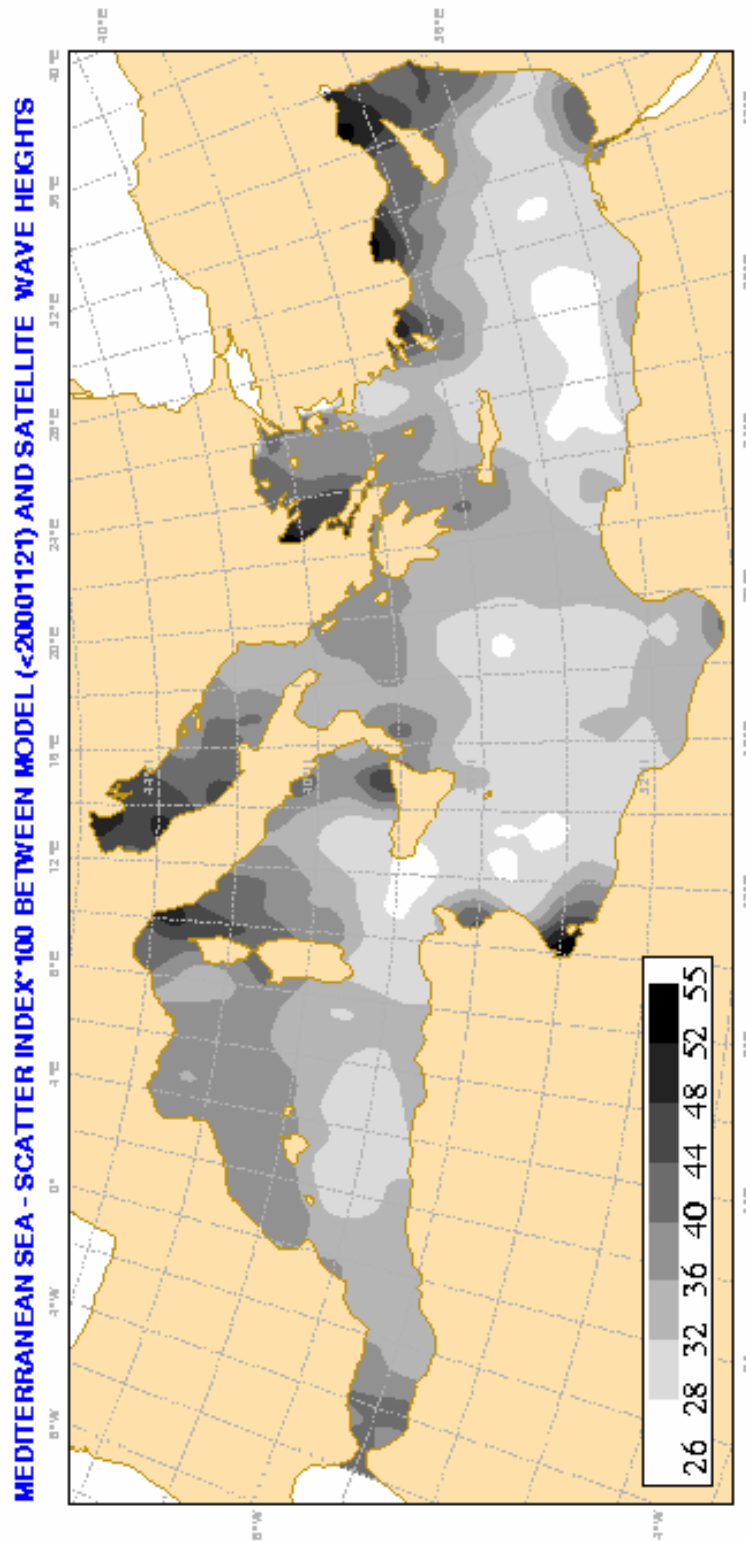


Figure 7 – Distribution of the scatter index of the best-fit between modelled and satellite measured wave heights. Figures are in percent.
The period considered is before 21 November 2000.

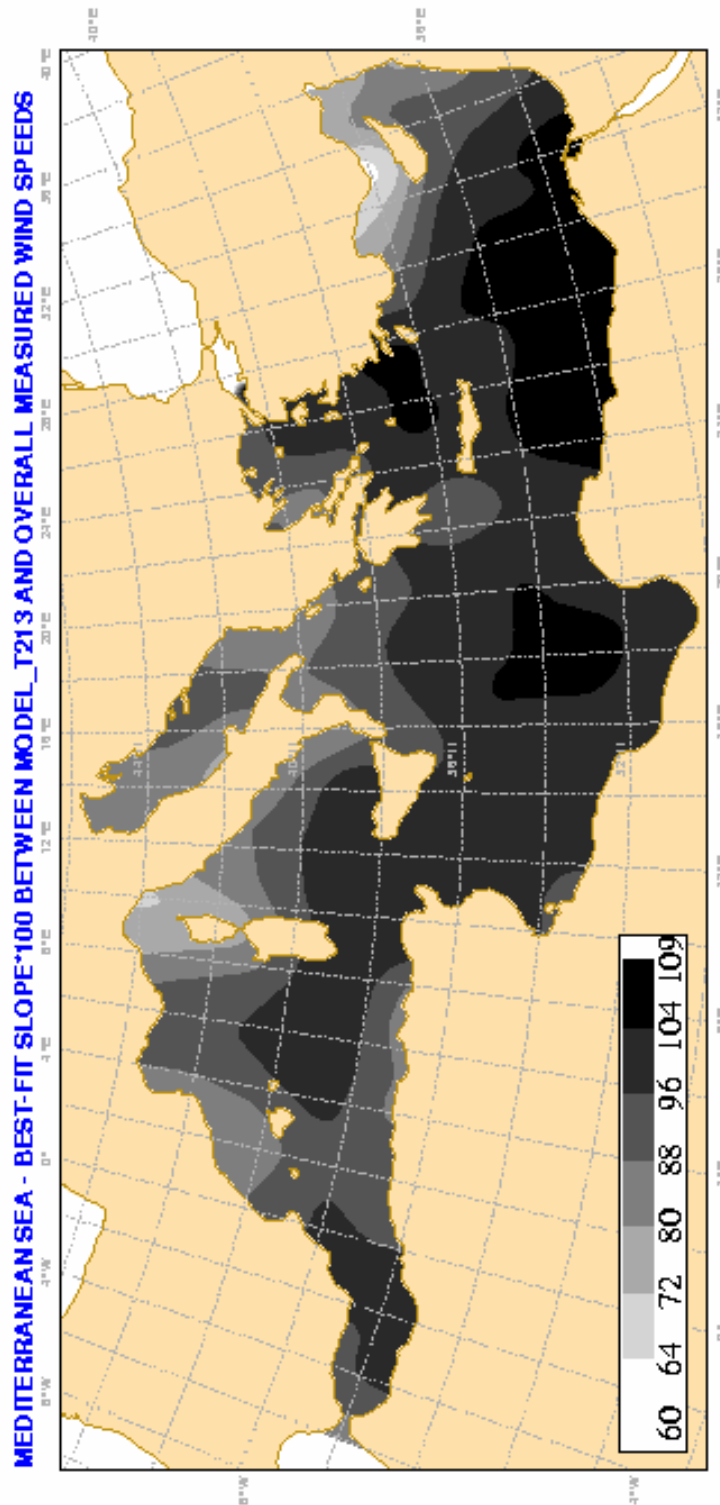


Figure 8 – Distribution of the best-fit slope between modelled and satellite measured wind speeds.

Figures are slope*100. The period considered is before 21 November 2000

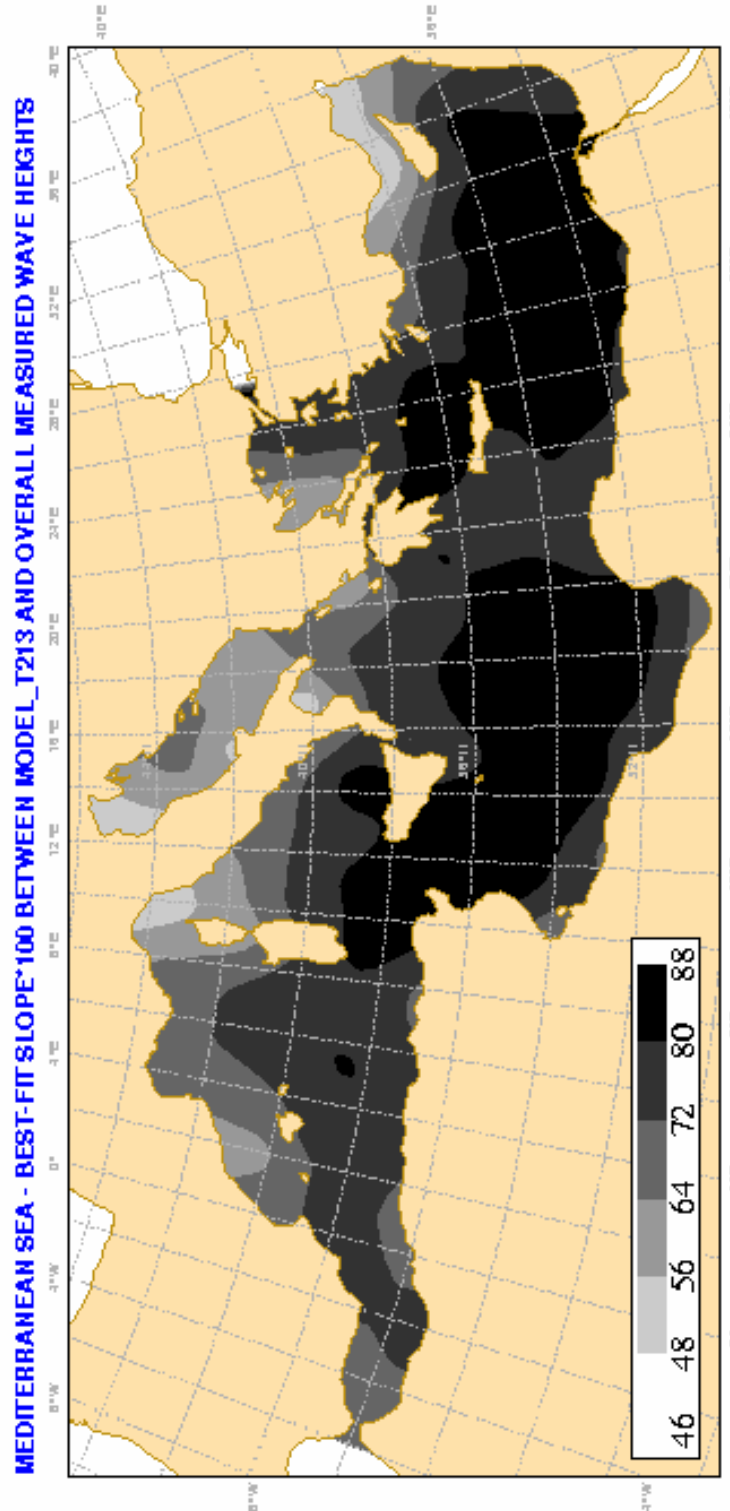


Figure 9 – Distribution of the best-fit slope between modelled and satellite measured wave heights.

*Figures are slope*100. The period considered is before 21 November 2000*

5. Statistical modelling and analysis of wind and waves

5.1. Short term and long term statistical modelling of wind and waves

The wind blowing over the sea is a turbulent flow field, involving a wide spectrum of length and time scales. The wind itself is modelled as a random (stochastic) field, and its study (both measurements and modelling) is performed through appropriate averaging procedures. The wind field over the sea is just the lower part of the atmospheric boundary layer, which is characterized by a smooth variation in the average (Cushman-Roisin, 1994; Sajjadi *et al*, 1999).

Sea waves are a complex phenomenon which is satisfactorily modelled as a stochastic field (Phillips 1977, Ochi 1998, Goda 2000). The wave field can be considered Gaussian, at least in offshore deep water areas. The local (in space and time) behaviour of sea waves, i.e. a sea state, can be modelled as a time-stationary and space-homogeneous Gaussian field, which is completely described by means of its directional spectrum $S(f, \mathbf{q})$. The latter provides the distribution of wave energy in the frequency f and direction \mathbf{q} domains, and, in practice, is usually given in discrete form, i.e.

$$\{S(f_\ell, \mathbf{q}_k), \quad \ell = 1, 2, \dots, L, \quad k = 1, 2, \dots, K\} \quad (1)$$

Using the spectrum $S(f, \mathbf{q})$, in conjunction with the theory of stochastic fields, various important wave parameters (also called spectral wave parameters) can be defined. The most common wave parameters are the significant wave height H_s , a mean wave period T_m ⁽¹⁾ and a mean wave direction Q_m ⁽²⁾. The definitions of these and other wave parameters in terms of the spectrum (spectral moments) will be given in Section 5.5.2.

Most of the wave parameters (e.g., H_s , T_m) can also be obtained by direct statistical analysis of wave records, or by means of remote sensing, without calculating the complete directional spectrum. In such cases, spectral models (parametric spectral functions) are available and can be used for the approximate reconstruction of either the frequency spectrum $S(f)$ or the directional spectrum $S(f, \mathbf{q})$. A minimum set of parameters required

⁽¹⁾ There are various different definitions of mean wave period. The symbol, T_m is used as a generic symbol for any (appropriate) mean wave period.

⁽²⁾ The previous footnote applies also to Q_m .

for a reliable reconstruction of $S(f)$ are H_s and T_m (or two others containing equivalent information). In addition, the knowledge of Q_m permits to obtain an approximate model for $S(f, \mathbf{q})$.

The directional spectrum, or an appropriate set of spectral parameters approximately defining the spectrum $S(f, \mathbf{q})$, constitutes the *short-term* description of the wave conditions.

Parametric models of frequency spectrum

Usually, parametric frequency spectra are considered unimodal. A general model of such a unimodal spectral density function is (see, e.g. Massel, 1996)

$$S(f) = Af^{-p} \exp(-Bf^{-q}), \quad (2)$$

where A , B , p , q are free parameters. In this case, the spectral moments are obtained in closed form, in terms of the spectral parameters and the Gamma function. More general, multimodal, frequency spectra, describing combined seas (e.g. wind sea and swell) can be defined as appropriate mixtures of the models (2). See, e.g., Ochi and Hubble (1976), Ochi (1998).

A most popular spectrum among the family (2) is the **Pierson-Moskowitz** spectrum (1964) for fully developed seas, in which $p=5$, $q=4$ and $B=5/4$ (see, e.g., Massel 1996, Sec. 3.2.2.2). In Naval Architecture, the two-parameter Bretschneider spectrum, which includes model (2) as a special case, is commonly used (Ochi 1998):

$$S(f) = \frac{1.25}{4} \frac{f_p^4}{f^5} H_s^2 \exp \left\{ -1.25 \left(\frac{f_p}{f} \right)^4 \right\}, \quad (3)$$

where $f_p = 1/T_p$ denotes the peak frequency.

The **JONSWAP** frequency spectrum (Hasselmann *et al* 1973) extends the Pierson-Moskowitz spectrum in fetch-limited seas, and is defined by

$$S(f, \mathbf{q}; H_s, T_p) = \left(\frac{a}{f^5} \exp \left[-1.25 \left(\frac{f}{f_p} \right)^4 \right] \right) \mathbf{g}^{d(f)}, \quad (4)$$

In the above formula, the parameter a is defined by means of the formula (Goda 2000),

$$\mathbf{a} = \frac{0.0624(1.094 - 0.01915 \ln \mathbf{g})}{0.23 + 0.0336\mathbf{g} - 0.185(1.9 + \mathbf{g})^{-1}} (H_s)^2 f_p^4, \quad (5)$$

where the parameter g and the function $d(f)$ are defined by

$$g = 3.3, \quad d(f) = \exp\left[-\frac{(f - f_p)^2}{2s_0^2 f_p^2}\right] \quad \text{where} \quad s_0 = \begin{cases} 0.07, & \text{for } f < f_p \\ 0.09, & \text{for } f \geq f_p \end{cases}. \quad (6)$$

It should be noted that the above model spectra are defined by means of basic wind and wave parameters considered in this Atlas. In the above formulations, the frequency spectrum is defined through the two parameters H_s , T_p . In the case of fully developed seas, the spectrum (3) is reduced to a single-parameter PM spectrum, by means of the formulae:

$$H_s = 0.2092 \frac{U_w^2}{g}, \quad T_p = 7.1628 \frac{U_w^2}{g}. \quad (7)$$

Thus, for fully developed seas, wind speed is the only parameter controlling the frequency spectrum (provided that a pure wind sea state is present – no swell).

A number of expressions exist for the swell frequency distribution, basically aiming at providing a more or less narrow peaked function (Massel, 1996). A careful assessment and testing of various candidate spectra, suggests that the following expression can be used:

$$S(f) = \frac{6m_0}{f_p} \left(\frac{f}{f_p}\right)^{-6} \exp\left[-1.2 \left(\frac{f}{f_p}\right)^{-5}\right], \quad (8)$$

where m_0 is the zero-th order moment of $S(f)$.

Based on a classification by Torsethaugen (1993, 1996), we define the overall sea state as being of either wind sea type or swell type, according to

$$\begin{aligned} T_p &\leq 6.6 H_s^{1/3} && \text{wind sea type} \\ T_p &> 6.6 H_s^{1/3} && \text{swell type} \end{aligned}$$

The type of sea state determines which formulation to use for the overall spectrum.

Parametric models of directional spectrum

Directional-spectrum models are obtained by combining a frequency spectrum with a directional spreading function. Usual models for the latter are the **cosine-power** model, the **hyperbolic cosine** model and the **Wrapped Gaussian** model (see, e.g. Massel, 1996, Sec.3.3).

The cosine-power model is given by

$$D(\Theta, s) = \frac{2^{2s-1}}{p} \frac{\Gamma^2(s+1)}{\Gamma(2s+1)} \cos^{2s}\left(\frac{\Theta - \Theta_p}{2}\right), \quad -p \leq \Theta \leq p, \quad (9)$$

where s is an empirical function and Θ_p is the direction corresponding to the peak frequency.

The hyperbolic-cosine spreading function (Donelan *et al* 1985), is usually used in conjunction with the JONSWAP frequency spectrum for modelling wind-sea and swell systems, from integrated wave parameters. In this case, the form of the directional model spectrum is

$$S(f, \mathbf{q}; H_s, T_p, \mathbf{Q}_m) = \left(\frac{a}{f^5} \exp \left[-1.25 \left(\frac{f}{f_p} \right)^{-4} \right] \mathbf{g}^d \right) \cdot D(\mathbf{q}; \mathbf{Q}_m), \quad (10)$$

where H_s, T_p, \mathbf{Q}_m are the significant wave height, the peak period, and the mean wave direction, respectively. The spreading function $D(\mathbf{q}; \mathbf{Q}_m)$ in Eq. (10) is defined as follows (Donelan *et al* 1985),

$$D(\mathbf{q}; \mathbf{Q}_m) = \frac{1}{2} \beta \cosh^{-2} [\beta (\mathbf{q} - \mathbf{Q}_m)], \quad (11)$$

where the parameter β is given by

$$\beta = \begin{cases} 2.61 (f / f_p)^{1.3}, & \text{for } 0.562 < f / f_p < 0.95 \\ 2.28 (f / f_p)^{-1.3}, & \text{for } 0.95 \leq f / f_p < 1.60 \\ 1.24, & \text{otherwise} \end{cases} \quad (12)$$

Long-term considerations

For design, planning, assessment of the long-term efficiency, and other applications, we have to characterize the wave conditions in the large either in time or in space or both. For example, the operability and safety of a fixed offshore platform is dependent on the long-term behavior of the waves at a given site. On the other hand, the operability and safety of a ship (or a fleet) sailing through the Mediterranean Sea is dependent on the long-term behavior of the sea states along the whole area of her operation.

The key element of the characterization of the wave conditions is the long-term probabilistic description of the wave parameters at any site of interest, and the geographical display of these results along the whole sea area. In this connection, we have to consider and analyze many-year wave data, that is, populations (or time series) of spectra $\{S^{(n)}(f, \mathbf{q}), n = 1, 2, \dots, N\}$, or appropriate spectral parameters $\{?^{(n)} = (\mathbf{L}_1^{(n)}, \mathbf{L}_2^{(n)}, \dots), n = 1, 2, \dots, N\}$.

The amount of data should be large enough so that both the statistical variability within a season and the seasonal variability within a year is clearly resolved. Moreover, the modeling should be flexible enough so that it incorporates additional features, such as over-year variability and trends. In Sec. 5.5 the long-term notion of the wave climate at a given site in the sea is discussed and a clear definition of it is proposed.

5.2. Description of the data samples

The wind and wave data samples used in MEDATLAS mostly came from ECMWF-WAM data fields. They were produced by means of a two-stage processing. At the first-stage, the ECMWF wave data (fields) were compared with *in situ* measurements (at some points) and satellite data (globally, but only for H_s). During this stage, a systematic bias was identified for the H_s (Cavaleri *et al*, 2000, 2002), which was resolved by appropriate calibration procedures as described in Chap. 4). At the second stage, the wind and wave fields were transformed to time series associated with specific offshore points. These time series, associated with the offshore data points, constitute the fundamental database for the wind and wave conditions, from which all statistical information about the wind and wave climate is obtained.

The structure of the original time series and of the final populations of wind and wave data used in this Atlas is described in detail below. In the time-series format, the original datasets are sequences of vectors of the form

$$\mathbf{z} = \mathbf{z}(\text{point}; \text{time}) = \mathbf{z}(p; y, m, d, h), \quad (1)$$

where p is the identifier of the geographical location, and (y, m, d, h) is the date/time identifier (y =year, m =month, d =day, h =hour of the day). Each vector \mathbf{z} contains initially 6 components, which after a preprocessing (see below) becomes 9,

$$\mathbf{z} = [z_1, z_2, \dots, z_N], \quad N=6, \quad (2)$$

describing various wind and wave parameters. Table 4 presents the first ten rows of \mathbf{z} , associated with the offshore point $p=(1^\circ \text{ W}, 36^\circ \text{ N})$, located in the south-eastern coast of Spain.

The first four columns appearing in Table 4 evaluate the date/time identifier (y, m, d, h) , which is considered as an argument (and not as a component) of \mathbf{z} . The remaining 6 columns define the 6 components of the vector \mathbf{z} , which are:

$z_1 = H_s$: significant wave height

$z_2 = \Psi$: mean wave direction according to WAM convention⁽³⁾

$z_3 = T_p$: peak period

$z_4 = T_e$: mean energy period

$z_5 = U_{10}$: horizontal wind component at 10m height over the quiet sea surface (W to E)

$z_6 = V_{10}$: vertical wind component at 10m height over the quiet sea surface (S to N)

⁽³⁾ According to WAM convention, waves coming from the North correspond to a mean direction $Y = 180^\circ$, and waves coming from the East correspond to a mean direction $Y = 270^\circ$.

Table 4 - WAM time-series data for the offshore point $p=(1^\circ W, 36^\circ N)$.

year	m	d	h	z_1	z_2	z_3	z_4	z_5	z_6
1992	7	1	0	1.39	73.91	5.20	4.64	6.84	4.09
1992	7	1	6	1.81	72.83	6.92	6.05	6.11	4.82
1992	7	1	12	1.47	77.61	6.92	6.19	4.84	1.72
1992	7	1	18	1.11	84.32	6.92	6.06	-0.24	0.30
1992	7	2	0	0.90	90.69	6.92	6.02	-2.95	0.44
1992	7	2	6	0.77	99.06	6.30	5.74	-5.67	-2.69
1992	7	2	12	1.03	09.55	4.30	4.49	-4.61	-5.26
1992	7	2	18	1.33	23.01	5.20	4.71	-6.49	-5.69
1992	7	3	0	1.07	25.22	5.73	5.21	-4.97	-0.47
1992	7	3	6	0.83	25.45	5.73	4.64	-3.89	-4.78
.....

A data set consisting of records of the type $\mathbf{z} = \mathbf{z}(p; y, m, d, h)$ contains information about

- The serial correlation of the sea states, and
- The joint probability structure of various wind and wave parameters.

First, a pre-processing was applied to the time-series data, including:

- Calculation of the speed $U_w = \sqrt{U_{10}^2 + V_{10}^2}$ of the wind at 10 m height, based on the two wind components.
- Calculation of direction Q_{wind} of the wind at 10 m height, based on the two wind components.
- Conversion of wind and wave directions from the WAM convention to the nautical convention⁽⁴⁾.

⁽⁴⁾ According to nautical convention waves coming from the North correspond to a mean direction $Q = 0^\circ$, and waves coming from the East correspond to a mean direction $Q = 90^\circ$. The conversion between WAM convention and nautical convention is made by means of the formulae: $Q = Y + 180^\circ$, if $0^\circ \leq Y < 180^\circ$, and $Q = Y - 180^\circ$, if $180^\circ \leq Y < 360^\circ$.

The derived data sets in the third stage, constitute the *samples* $X(p; y, m, d, h)$ stored in MEDATLAS database:

$$X(p; y, m, d, h) = [H_s, Y, T_p, T_{-10}, U_{10}, V_{10}, U_w, Q_{wind}, Q_{wave}]. \quad (3)$$

As an example, Table 5 presents the first twelve rows of X –type data associated with the offshore point $p=(1^\circ \text{ W}, 36^\circ \text{ N})$, located in the south-eastern coast of Spain.

Table 5 - Processed time series for the offshore point $p=(1^\circ \text{ W}, 36^\circ \text{ N})$.

<i>year</i>	<i>m</i>	<i>d</i>	<i>h</i>	H_s	Y	T_p	T_{-10}	U_{10}	V_{10}	U_w	Q_{wind}	Q_{wave}
1992	7	1	0	1.39	73.91	5.20	4.64	6.84	4.09	7.97	239.12	253.91
1992	7	1	6	1.81	72.83	6.92	6.05	6.11	4.82	7.78	231.73	252.83
1992	7	1	12	1.47	77.61	6.92	6.19	4.84	1.72	5.14	250.44	257.61
1992	7	1	18	1.11	84.32	6.92	6.06	-0.24	0.30	0.38	141.34	264.32
1992	7	2	0	0.90	90.69	6.92	6.02	-2.95	0.44	2.98	98.48	270.69
1992	7	2	6	0.77	99.06	6.30	5.74	-5.67	-2.69	6.28	64.62	279.06
1992	7	2	2	1.03	09.55	4.30	4.49	-4.61	-5.26	6.99	41.23	29.55
1992	7	2	8	1.33	23.01	5.20	4.71	-6.49	-5.69	8.63	48.76	43.01
1992	7	3	0	1.07	25.22	5.73	5.21	-4.97	-0.47	4.99	84.60	45.22
1992	7	3	6	0.83	25.45	5.73	4.64	-3.89	-4.78	6.16	39.14	45.45
.....

5.3. From original samples to grouped samples

All wind and wave parameters considered in MEDATLAS, except the peak period T_p (see section 5.3.3, below), can be considered as continuously distributed random variables. Their probabilistic description is inferred by means of appropriate statistical processing of the available samples, stored in the MEDATLAS database. Although not necessary, it is common practice (also followed herewith) to proceed by first grouping the observations with the aid of a partition Ξ of the sample space, replacing, in this way, the original sample, say

\mathbf{X} , by the grouped sample, say $\mathbf{X}_g = \mathbf{X}_g(\Xi)$.

Especially, the partitions of the univariate and bivariate grouped samples are defined as follows

$$\text{Univariate case: } \Xi = \{0 = \mathbf{x}_0 < \mathbf{x}_1 < \mathbf{x}_2 < \dots < \mathbf{x}_i < \dots < \mathbf{x}_I\}, \quad \mathbf{x}_I \geq X_{\max}, \quad (1a)$$

$$\text{Bivariate case: } \Xi = \{[\mathbf{x}_{i-1}^1, \mathbf{x}_i^1] \times [\mathbf{x}_{j-1}^2, \mathbf{x}_j^2], \quad i = 1, 2, K, I, \quad j = 1, 2, K, J\}. \quad (1b)$$

The center of the cells are denoted by x_i (univariate case) and (x_{ij}^1, x_{ij}^2) (bivariate case) and the area of the bivariate cell by $DA_{ij} = DX_i^1 \times DX_j^2$, where $DX_i^1 = x_i^1 - x_{i-1}^1$, $i = 1, 2, K, I$, and $DX_j^2 = x_j^2 - x_{j-1}^2$, $j = 1, 2, K, J$.

Thus, by means of partitions (1a,b), the univariate and bivariate grouped samples are defined as follows

$$\text{Univariate case: } \mathbf{X}_g = \mathbf{X}_g(\Xi) = ((x_1, \mathbf{n}_1), (x_2, \mathbf{n}_2), \dots, (x_i, \mathbf{n}_i), \dots, (x_I, \mathbf{n}_I)), \quad (2a)$$

$$\text{Bivariate case: } (\mathbf{X}_g^1, \mathbf{X}_g^2) = (\mathbf{X}_g^1, \mathbf{X}_g^2)_X = \{((x_i^1, x_j^2), \mathbf{n}_{ij}), \quad i = 1(1)I, \quad j = 1(1)J\} \quad (2b)$$

where \mathbf{n}_i are the frequencies of occurrence of the events $[\mathbf{x}_{i-1} \leq X < \mathbf{x}_i]$, and \mathbf{n}_{ij} are the frequencies of occurrence of the events $[X^1 \in [\mathbf{x}_{i-1}^1, \mathbf{x}_i^1] \wedge X^2 \in [\mathbf{x}_{j-1}^2, \mathbf{x}_j^2]]$.

The univariate and bivariate empirical probability density function (EPDF), denoted respectively by $f_{\Xi}(x)$ and $f_{\Xi}(x_1, x_2)$ are defined, in terms of the grouped sample, as follows:

$$f_{\Xi}(x) = \begin{cases} 0, & x < 0, \\ \frac{\mathbf{n}_i}{N\Delta x_i}, & \mathbf{x}_{i-1} \leq x < \mathbf{x}_i, \\ 0, & x \geq \mathbf{x}_I. \end{cases} \quad f_{\mathbf{X}}(x^1, x^2) = \begin{cases} 0 & x^1 < 0, \quad x^2 < 0, \\ \frac{\mathbf{n}_{ij}}{NDA_{ij}}, & (x^1, x^2) \in [\mathbf{x}_{i-1}^1, \mathbf{x}_i^1] \times [\mathbf{x}_{j-1}^2, \mathbf{x}_j^2], \\ 0 & x^1 \geq \mathbf{x}_I^1 \quad \text{or} \quad x^2 \geq \mathbf{x}_I^2, \end{cases} \quad (3)$$

The various statistical moments can be calculated either from the original samples (time series) or from the grouped samples. The following table presents the corresponding definitions:

– Univariate case

	Grouped sample	Initial sample	
a) Mean value	$\bar{x}_g \equiv \bar{x}_g(\Xi) = \frac{1}{N} \sum_{i=1}^I n_i x_i,$	$\bar{X} = \frac{1}{I} \sum_{i=1}^I X_i,$	(4)
b) Variance	$\bar{s}_g^2 \equiv \bar{s}_g^2(\Xi) = \frac{1}{N} \sum_{i=1}^I n_i (x_i - \bar{x}_g)^2,$	$S^2 = \frac{1}{I} \sum_{i=1}^I (X_i - \bar{X})^2,$	(5)
c) Skewness	$m_{3,g} \equiv m_{3,g}(\Xi) = \frac{1}{N} \sum_{i=1}^I n_i (x_i - \bar{x}_g)^3,$	$m_3 = \frac{1}{I} \sum_{i=1}^I (X_i - \bar{X})^3,$	(6)
d) Kurtosis	$m_{4,g} \equiv m_{4,g}(\Xi) = \frac{1}{N} \sum_{i=1}^I n_i (x_i - \bar{x}_g)^4,$	$m_4 = \frac{1}{I} \sum_{i=1}^I (X_i - \bar{X})^4,$	(7)

– Bivariate case

	Grouped sample	Initial sample	
a) Mean values	$\bar{x}_g^1(\mathbf{X}) = \frac{1}{N} \sum_{i=1}^I n_{ij} x_i^1, \quad \bar{x}_g^2(\mathbf{X}) = \frac{1}{N} \sum_{j=1}^J n_{ij} x_j^2,$	$\bar{X}^1 = \frac{1}{I} \sum_{i=1}^I X_i^1, \quad \bar{X}^2 = \frac{1}{I} \sum_{i=1}^I X_i^2,$	(8)
b) Second-order central moments	$m_g^{ab}(\mathbf{X}) = \frac{1}{N} \sum_{i=1}^I \sum_{j=1}^J n_{ij} (x_i^a - \bar{x}_g^a)(x_j^b - \bar{x}_g^b),$ $a, b = 1, 2$	$m^{ab} = \frac{1}{I} \sum_{i=1}^I (X_i^a - \bar{X}^a)(X_i^b - \bar{X}^b),$ $a, b = 1, 2$	(9)
c) Correlation coefficient.	$r = \frac{m_g^{12}}{\sqrt{m_g^{11} m_g^{22}}}$	$r = \frac{m^{12}}{\sqrt{m^{11} m^{22}}}.$	(10)

Clearly, the partition Ξ should be fine enough so that the moments calculated in terms of the grouped sample to be in good agreement with the moments calculated from the original sample (criterion of moments, see below).

The *advantages* of grouping of time series data are:

- (i) a piecewise constant estimate for the probability density function can be realised, and
- (ii) the amount of arithmetic operations required in performing statistical estimation is reduced.

On the other hand, the replacement of the original sample by the grouped sample has the important disadvantage that the available information concerning the probability structure of the population under study is artificially reduced.

The coarser the partition is, the smaller the information content of the grouped sample $\mathbf{X}_g(\Xi)$ becomes. As a consequence, a grouped sample $\mathbf{X}_g(\Xi)$ corresponding to a coarse partition Ξ may be of little statistical importance, giving a rough description of the probability structure of the examined population. Accordingly, the question of how to select an *appropriate* (or an *optimal*) partition Ξ for a given sample of a (continuously distributed population) is of great importance, and will be briefly discussed below.

5.3.1. Criteria for data grouping

(Ivchenko and Medvedev 1990, Aivazian et. al. 1986)

I. *The criterion of equiprobable cells*

An appropriate partition Ξ should be such that the probability mass that corresponds to each cell in the main part of the sample space (i.e., excepting the tails) to be comparable.

II. *The criterion of moments*

An appropriate partition Ξ should be fine enough so that the mean, the variance, the skewness and the kurtosis of the corresponding grouped sample are almost the same with the corresponding quantities calculated from the original sample. (Higher order moments can also be included in this criterion).

III. *The criterion of the maximum likelihood estimator*

An appropriate partition Ξ should be fine enough so that the model parameters estimated by means of the ML-estimator based on the original sample is almost the same as the model parameters estimated by means of the ML-estimator based on the grouped sample. This criterion can be used only when a satisfactory probability model has been selected prior to the grouping.

IV. *The information criterion*

An appropriate partition Ξ should be fine enough so that the number I of cells satisfies the inequality: $I > \log_2 N + 1$, where N is the sample size. See Aivazian et al. (1986, Section 5.4.2).

V. *The criterion of relative accuracy*

In the case where it is known *a priori* that the sample values, are recorded with an accuracy

ϵ (if, e.g., we keep only one decimal digit, then $\epsilon=0.1$) then, the appropriate partition should be coarse enough so that the minimum length of the cells is considerably greater than ϵ .

All criteria stated above have been taken into account in MEDATLAS for selecting partitions for the continuously distributed variables considered (see Sec. 5.2). It should be noted, however, that the problem of selecting an appropriate partition does not always have a unique solution and, in any case, a trial-and-error procedure, taking into account the above criteria, is the only "general" method for finding a sufficiently good solution.

5.3.2. Partitions of wind and wave parameters

After a considerable amount of numerical investigation, and taking into account the geographical area considered in MEDATLAS, the following partitions have finally been decided for the parameters U_w , Q_{wind} , H_s , Q_{wave} :

Table 6 - Partitions for wind and wave parameters

Parameters	Range	No. of Cells	Partition
U_w (m/sec)	0-20	15	0(1)10, 10(2)20 +
Q_{wind} (degrees) nautical convention	-7.5-352.5	24	-7.5(15)352.5
H_s (m)	0-10	17	0(0.25)2, 2(0.5)4, 4(1)6, 7.5, 9 +
Q_{wave} (degrees) nautical convention	-7.5-352.5	24	-7.5(15)352.5

5.3.3. On the partition of the peak period T_p

The sample space of WAM data for T_p is **discrete**, although the variable T_p should be considered as a continuously distributed one, like all other wind and wave parameters. This is due to the fact that the WAM data for T_p are given using predetermined bins.

This is a delicate and, in fact, *artificial* problem. Since there are no data between bins, the appearance of the histograms is very sensitive to the definition of cells. In fact, we can obtain infinitely many (and *essentially different*) variants of a T_p -histogram corresponding to a given WAM time series for T_p , by "slightly" changing the limits of the cells.

The above problem has been tackled in a previous project (WERATLAS, Athanassoulis and Stefanakos 1996a), and the solution proposed is to devise and apply a definite and

reasonable principle permitting to uniquely define the T_p partition. This solution has also been adopted in MEDATLAS. The basic conventions underlying the definition of the cells for T_p are the following:

- **C1.** 1 bin corresponds to 1 cell,
- **C2.** The points separating successive cells are the midpoints between successive bins.
- **C3.** The first and the last bins lie at the centre of the first and last cells, respectively.

Convention 3 is necessary in order to define uniquely (and reasonably) minimum and maximum values, i.e. the range for T_p . It is easy to verify that conventions C1-C3 define T_p - cells *uniquely*. Moreover, this procedure is *correct* under the reasonable assumption that the "real" values of T_p are (approximately) uniformly distributed between successive bins and they are "attracted" by the nearest bin existing in WAM model. Using the above conventions, we arrived at the following partition for T_p :

Table 7 - Partition for the peak period

Parameters	Range	No. of Cells	Partition
T_p (sec)	0 ÷ 20.9	19	{0, 1.93, 2.58, 3.12, 3.78, 4.57, 5.03, 5.53, 6.08, 6.69, 7.36, 8.10, 8.90, 9.79, 10.78, 11.86, 13.04, 14.35, 17.36, 20.91}

5.4. Analytic probability models

The long-term (climatic) distributions of the various wind and wave parameters are usually represented by means of analytic probability models. For the distribution of wind speed, the most commonly used model is the Weibull distribution. Next, for the significant wave height and the distributions of the various wave periods the most widely used probability model is the lognormal pdf (Jasper 1956, Ochi 1978, Haver 1985, Guedes Soares *et al* 1988, Athanassoulis *et al* 1994, Athanassoulis and Stefanakos 1996). Besides, other probability models have also been used as, e.g., the Weibull pdf (Nordenstrom 1969, Krogstad 1985, Bitner-Gregersen and Cramer 1995), the generalised Gamma pdf (Andrew and Price 1978), and the modified log-normal pdf including correction for skewness (Fang and Hogben 1982). On the other hand, there have not been used parametric probability models for the mean (wind and wave) direction, probably because of the complicated form of the corresponding empirical pdf (for example, direction is often bimodal).

The situation becomes much more complicated if we turn to the most important bivariate (multivariate) case. Note that, the versatility of parametric multivariate models is rather

restricted, and the construction of a new parametric model having pre-specified features is far from being an easy task. For modelling the probability distribution of (H_s, T_m) ⁵, the bivariate lognormal pdf was first proposed by Ochi (1978) and has been widely used. A modified bivariate lognormal distribution was introduced later by Fang and Hogben (1982), improving the performance of the modelling. The bivariate Gamma pdf was extensively studied by Gran (1992), who commented on its possible application to (H_s, T_m) data, without giving specific examples. The bivariate Weibull pdf (a special case of Gran's Gamma model) has been applied to (H_s, T_m) data by Mathiesen and Bitner-Gregersen (1990), who also presented a comparison of the three different parametric bivariate models mentioned above and the conditional-distribution approach (see below). A more versatile bivariate pdf, the Plackett model, was introduced by Athanassoulis *et al* (1994) and was successfully applied to (H_s, T_m) and other pairs of data by the authors and other researchers (Monbet *et al* 1995, Feld and Wolfram 1996). An important feature of the Plackett model is that its univariate marginals can be of any type, the model itself providing a parametric correlation pattern permitting any correlation coefficient $r \in [-1, 1]$.

A general method of analytic representation of the empirical pdf of bivariate and multivariate data is the conditional-distribution approach. This method has been extensively used for bivariate (H_s, T_m) data (see, e.g., Dacuncha, Hogben and Andrews 1984, Fang *et al* 1989, Mathiesen and Bitner-Gregersen 1990, Bitner-Gregersen, *et al* 1998), as well as for trivariate (H_s, T_m, U_{wind}) data (Belberova and Myrhaug 1996). However, only one marginal is directly controlled by the corresponding marginal data. All other marginals are computed by integration from the multivariate model and may exhibit discrepancies when compared with the marginal data.

The use of many different parametric pdfs (including the conditional-distribution approach) for modelling the long-term distributions of one and the same metocean parameter, dramatically reflects two controversial issues. On the one hand, there are no theoretical grounds to justify the type of distribution of any of the above parameters. On the other hand, there is a strong desire to construct and have at our disposal analytic probability models for the distributions of the various parameters. The availability of an analytic expression for the probability density function is an indispensable prerequisite for many important applications such as, e.g., the extrapolation to calculate extreme values or the integration to calculate cumulative long-term quantities. In the multivariate case, the availability of an analytic probability model is important even for purely exploratory purposes (visualization).

All metocean parameters can be modelled as continuous random variables. In most cases, the natural support is the non-negative real axis $(0, \infty)$. Especially for the wave slope, the support must be restricted to a bounded interval, e.g. $(0, 10\%)$, because of wave breaking. Finally, all types of mean direction are circular random variables with support $[0, 2\pi)$ in rad, or $[0^\circ, 360^\circ)$ in degrees. The natural support of each metocean parameter (random variable) is of major importance in selecting and/or developing appropriate probability models.

⁵ Let us remind that, the symbol T_m is used as a generic symbol for any (appropriate) mean wave period.

An efficient general method for analytic representation of any wind or wave parameter (or any combination of them) is the *Kernel Density Model (KDM)* representation, which has been developed and assessed by Athanassoulis and Belibassakis (2002). In this work, a modification of the classical kernel density estimation method has been introduced that can serve the purpose of both estimation and analytic representation of any metocean parameter (the univariate case) or any set of metocean parameters (the multivariate case), provided that a representative histogram is available.

The kernel density model has been first introduced in the context of nonparametric discriminant analysis by Fix and Hodges (1951) and has become a central topic in the context of nonparametric statistical estimation and regression since the 1970's; see, e.g., the informative books by Silverman (1986) and Scott (1995).

In the case of a grouped sample, the kernel density model is (Athanassoulis and Belibassakis 2002)

$$f(x) = \frac{1}{N} \sum_{i=1}^I n_i K(x; x_i, h), \quad (1)$$

where v_i is the relative frequency of the bin x_i (i.e., the cell $[x_{i-1}, x_i)$), and $K(x; x_i, h)$ are smooth, non-negative functions, usually taken to be probability density functions in themselves, and h is a parameter controlling the bandwidth (essential support) of each $K(x; x_i, h)$. The functions $K(x; x_i, h)$ are called kernels and their specific form does not seriously affect the representation, except in the vicinity of the boundary points of the support of $f(x)$.

The fixed-bandwidth kernel representation has been found susceptible to local oversmoothing behaviour in the areas of high pdf values, and local undersmoothing behaviour in areas of low pdf values, especially in the tails of the represented pdf. Instead, the *variable-bandwidth kernel* representation of the form

$$f(x) = \frac{1}{N} \sum_{i=1}^I n_i K(x; x_i, h_i), \quad (2)$$

has been chosen. The local bandwidths h_i are associated one-to-one with the bins x_i .

The kernel density model can be extended in a straightforward way to the multivariate case; see, e.g., Silverman(1986), Hardle (1991), Wand and Jones (1995). Especially, in the bivariate case, given the grouped sample $\{(x_i^1, x_j^2), n_{ij}\}_{i=1(1)I, j=1(1)J}$, the variable-bandwidth kernel representation is defined by

$$f(x^1, x^2) = \frac{1}{N} \sum_{i=1}^I \sum_{j=1}^J n_{ij} K(x^1, x^2; (x_i^1, x_j^2), \mathbf{h}_{ij}). \quad (3)$$

If the elements of the bandwidth matrix are assumed to be pairwise independent and

uniform along x^1 and x^2 , a *multiplicative kernel* can be used

$$K(x^1, x^2; (x_i^1, x_i^2), \mathbf{h}_i) = K_1(x^1; x_i^1, h_i^1) K_2(x^2; x_i^2, h_i^2), \quad (4)$$

which is marginally consistent. Thus, the estimation of the bandwidths $h_{i_d}^d$ can be based on the marginal data alone.

Taking into account the different support of the various variables considered, new families of skewed (asymmetric) kernel functions are developed, suitable for the representation of the pdf's of linear random variables with support on $(0, \infty)$ or $(0, s)$, and of directional (circular) random variables with support on $[0^\circ, 360^\circ)$. The kernel functions considered are the univariate *Gamma*, Lognormal, Beta and *Wrapped Gaussian* kernels. Special attention has also been paid to the construction of bivariate kernels as tensor products of the univariate ones, which are able to represent any bivariate (and, in general, multivariate) empirical pdf, perfectly conforming with all marginals.

MATLAB codes are available upon request.

5.5. Wind and wave climate in the Mediterranean Sea

The wind and wave climate at a specific site in the sea can be defined by means of the long-term statistics of the (most) important wind and wave parameters. Traditionally, the time-series structure of wind and wave parameters is ignored and the latter are treated, in the long-term sense, as random variables. However, the seasonal inhomogeneity is important for most applications and should be taken into account. A way to do this is by subdividing the whole population into classes, according to the season (or month); this is a common practice in Wind and Wave Atlases; see, e.g., the ones developed by Naval Oceanography Command Detachment (1983), Hogben et al (1986), Direccion General de Puertos y Costas (1988), Athanassoulis and Skarsoulis (1992). See, also Hogben (1990). Accordingly, the wind and wave climate at a given site in the sea is defined by means of the *seasonal statistics* of the *important wind and wave parameters*. A more complete definition is

The *wind and wave climate* of a given site in the sea is defined by the set of the joint probability distributions of all important wind and wave parameters, including at least

i) The bivariate probability distributions:

$$P(U_W, \mathbf{Q}_{wind} \mid \text{site, season}),$$

$$P(H_S, T_p \mid \text{site, season}), P(H_S, \mathbf{Q}_{wave} \mid \text{site, season}),$$

$$P(H_S, U_W \mid \text{site, season}),$$

from which one can also derive:

ii) The corresponding univariate probability distributions:

$$P(U_W \mid \text{site, season}), P(\mathbf{Q}_{wind} \mid \text{site, season}),$$

$$P(H_S \mid \text{site, season}), P(T_p \mid \text{site, season}), P(\mathbf{Q}_{wave} \mid \text{site, season}),$$

iii) The mean seasonal (monthly) values of:

$$U_w, Q_{wind}, H_s, T_p, Q_{wave}.$$

Two different alternatives are commonly used regarding the seasonal resolution:

(i) The standard three-month seasons

Winter:	December, January, February
Spring:	March, April, May
Summer:	June, July, August
Autumn:	September, October, November

(ii) The monthly resolution

January
February
...
December.

Although all statistical analysis has been performed using the monthly resolution, due to space limitation, the results will be presented on a three-month seasonal basis.

A more modern approach is to treat long-term wind and wave data as time series and model them as random processes (Athanasoulis et al. 1992, Athanasoulis and Stefanakos 1995, Ochi 1998, Stefanakos 1999), exhibiting random variability, serial correlation and seasonal (statistical) periodicity. Since this approach is beyond the scope of the present Atlas, only some (sample) results of the seasonal variability will be shown here.

Moreover, the spatial distributions of the mean values of wind and wave parameters are examined and displayed as contour lines on the map of the Mediterranean Sea. A similar analysis and geographical display has been performed for the spatial distribution of the probability of occurrence of some important events.

5.5.1. Wind statistics

Two wind parameters have been considered:

– Wind speed at 10m height above the sea level

$$U_w = \sqrt{U_{10}^2 + V_{10}^2},$$

– Direction of wind at 10m height above the sea level

$$\Theta_{wind} = \tan^{-1} \left(\frac{V_{10}}{U_{10}} \right).$$

In Figure 10a-b, examples of univariate statistics at a specific datapoint (site) are given. The empirical density function of the wind speed U_w is usually well approximated by a Weibull distribution. The KDM representation can also be used, being a more flexible and generic model. Both models are plotted in Figure 10a (dashed line: Weibull, solid line: KDM). The empirical distribution of the wind direction is a circular random variable with a shape strongly dependent on the site and season. No simple analytical model can fit this distribution. Only the circular KDM representation can be used in all cases.

Similar results for any other point can be obtained using the histogram data provided by this Atlas and any appropriate graphical toolbox. In Part B, seasonal bivariate histograms of (U_w, θ_{wind}) are given for 129 points.

In Figure 11, examples of the spatial distribution of wind speed and wind direction are shown. The contours on each map of the first type, e.g. Figure 11a, are the locus of sites where the (seasonal) mean value of wind speed is constant. The corresponding value of the mean wind speed is depicted on each contour.

In maps displaying wind direction, e.g. Figure 11b, arrows show the direction from which wind blows (FROM definition). In interpreting and exploiting the charts of wind directionality, the following facts should be taken into account:

- a) Only directions corresponding to wind speed greater than 6m/s are considered,
- b) Only directions with frequencies greater than 10% are presented,
- c) The length of each arrow is proportional to the frequency of occurrence.

That is, these charts show the seasonal wind patterns associated with “strong” (greater than 6m/s) and “frequent” (greater than 10%) wind conditions.

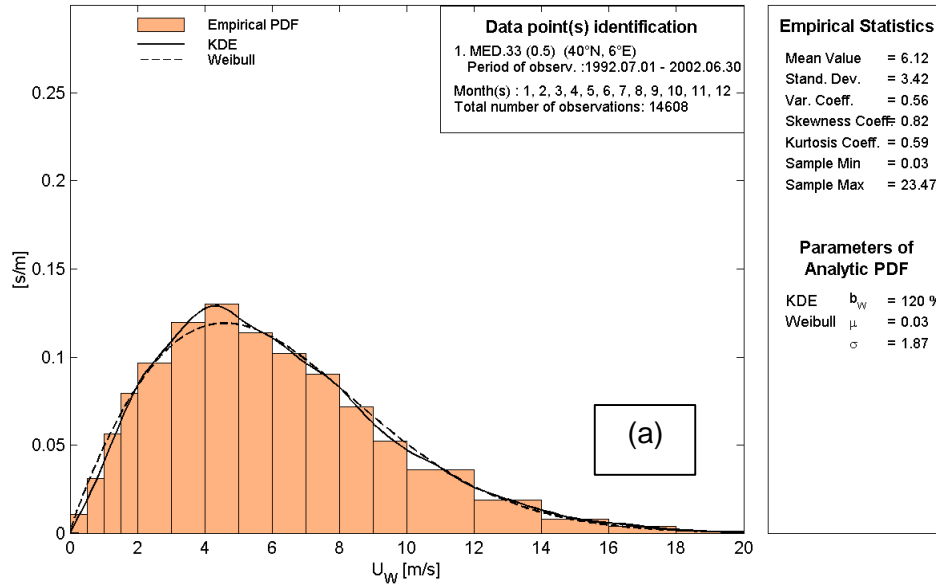
In Figure 12, examples of the spatial distribution of the following important events are given:

- i) the probability that $U_w < 4$ m/s
- ii) the probability that $U_w < 6$ m/s
- iii) the probability that $U_w > 8$ m/s
- iv) the probability that $U_w > 11$ m/s

The contours on each map represent curves of constant probability value for each event.

A complete set of this kind of results (maps) is given in Part B. There are “in total” 30 maps displaying the geographical distribution of wind parameters.

Probability density function of wind speed U_W



Polar histogram (%) of mean wind direction Θ_{wind}

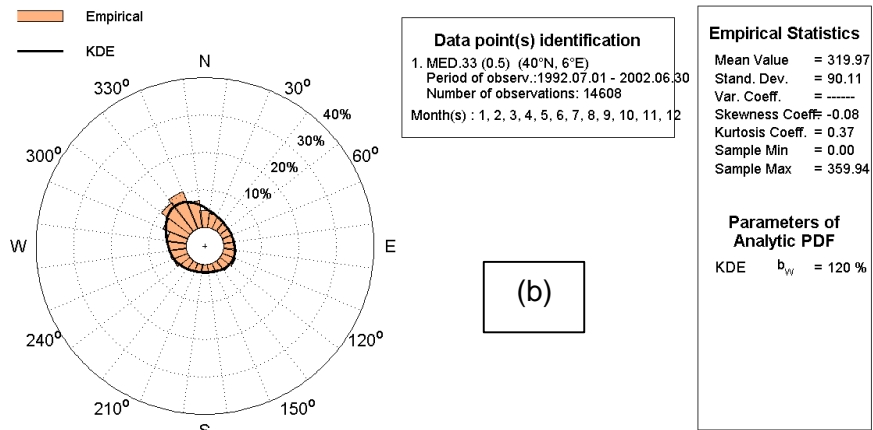


Figure 10 - Examples of wind statistics for datapoint (6E,40N). (a) Wind speed, (b) Wind direction.

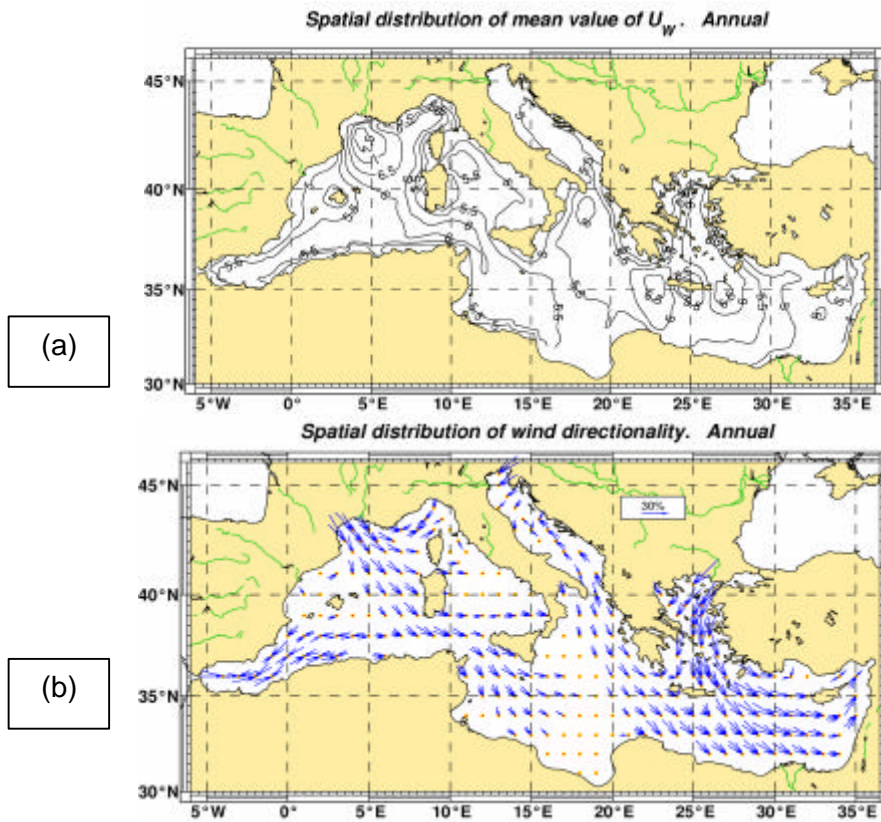


Figure 11 - Examples of spatial wind statistics. (a) Wind speed, (b) Wind direction.

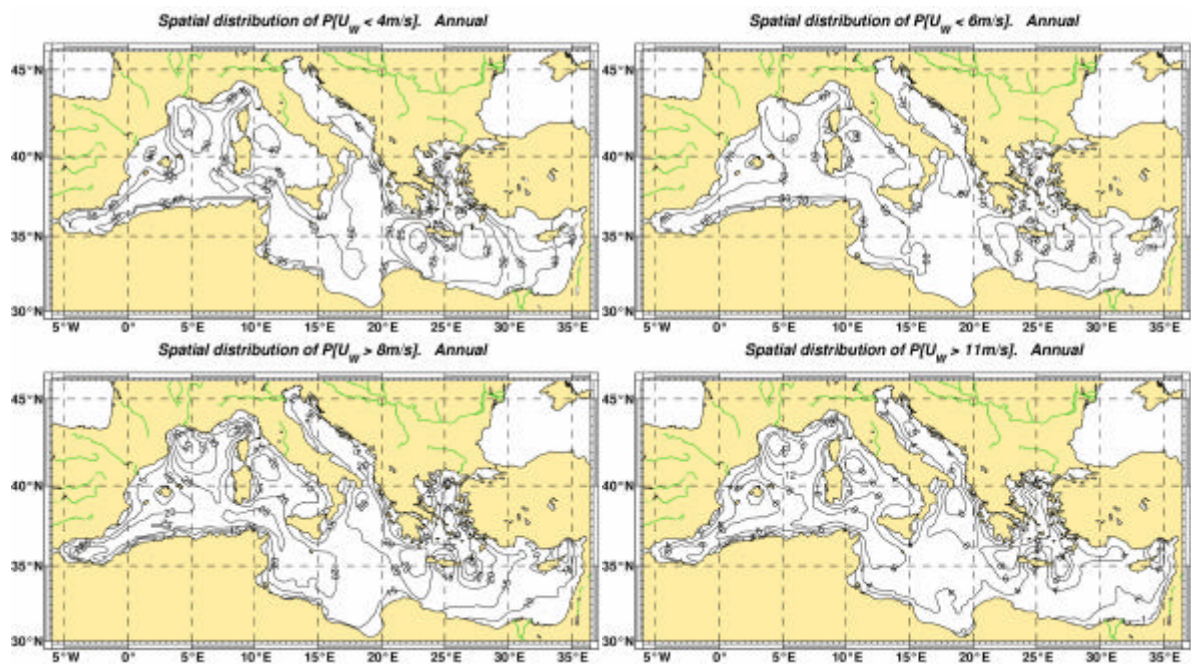


Figure 12 - Examples of spatial distribution of some important wind events

5.5.2. Wave statistics

The following wave parameters have been considered:

- Significant wave height

$$H_s = 4\sqrt{m_0}$$

- Peak period⁶

$$T_p = \frac{1}{f_p}, \quad \frac{dS(f_p)}{df} = 0$$

- Wave slope (based on the peak period)

$$b_p = \frac{2pH_s}{gT_p^2}$$

- Wave direction: Only KDM have been fitted due to the circular character of the pdf

$$T_{\text{wave}} = \arctan \left(\frac{\int_0^{2p} \int_0^{\infty} S(f, \mathbf{q}) \sin \mathbf{q} df d\mathbf{q}}{\int_0^{2p} \int_0^{\infty} S(f, \mathbf{q}) \cos \mathbf{q} df d\mathbf{q}} \right)$$

In Figure 13a-d, examples of univariate statistics at a specific datapoint (site) are given. The empirical density functions of the significant wave height and peak period are usually well approximated by a Lognormal distribution. The KDM representation can also be used, being a more flexible and generic model. Both models are plotted in Figure 13a-b (dashed line: Lognormal, solid line: KDM). The empirical distribution of the wave slope (based on the peak period) is successfully approximated by the KDM (Barstow *et al*, 2001); see, e.g., Figure 13c. The empirical distribution of the wave direction is a circular random variable with a shape strongly dependent on the site and season. It is usually multimodal, and no simple analytical model can fit this distribution. Only the circular KDM representation can be used in all cases; see Figure 13d.

Similar results for any other point can be obtained using the histogram data provided by this Atlas and any appropriate graphical toolbox. In Part B, seasonal bivariate histograms of (H_s, T_p) and $(H_s, \theta_{\text{wave}})$ are given for 129 points.

In Figure 14a-c, examples of the spatial distribution of significant wave height, peak period, and wave slope are shown. The contours on each map are the locus of sites where the (seasonal) mean value is constant.

In maps displaying wave direction, e.g. Figure 14d, arrows show the direction from which

⁶ This theoretical definition is not in full agreement with the peak period (frequency) calculated by WAM. The latter calculates spectral ordinates at prespecified frequency bins and provides as f_p , the bin-value corresponding to the maximum spectral value.

waves comes (FROM definition). In interpreting and exploiting the charts of wave directionality, the following facts should be taken into account:

- a) Only directions corresponding to wave heights greater than 1m are considered,
- b) Only directions with frequencies greater than 10% are presented,
- c) The length of each arrow is proportional to the frequency of occurrence.

That is, these charts show the seasonal wave patterns associated with “strong” (greater than 1m) and “frequent” (greater than 10%) wave conditions.

In Figure 15, examples of the spatial distribution of the following important events are given:

- i) the probability that $H_s < 0.5$ m
- ii) the probability that $H_s < 1.25$ m
- iii) the probability that $H_s > 2.5$ m
- iv) the probability that $H_s > 4$ m

The contours on each map represent curves of constant probability value for each event.

A complete set of this kind of results (maps) is given in Part B. There are “in total” 40 maps displaying the geographical distribution of wave parameters.

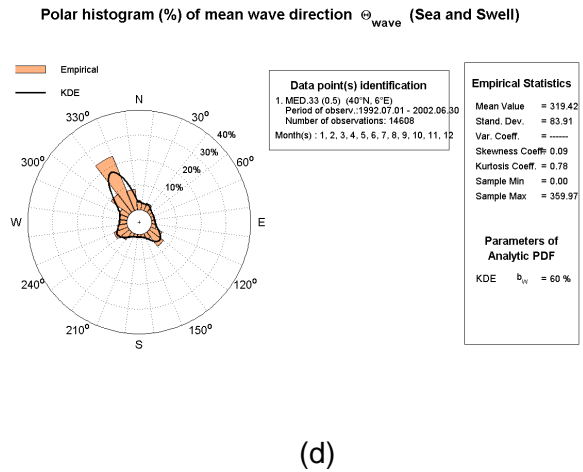
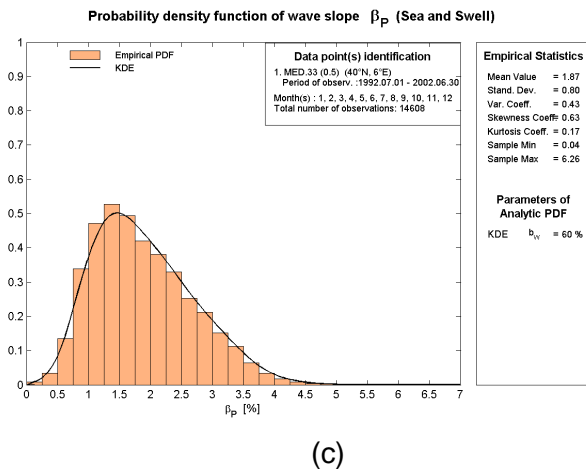
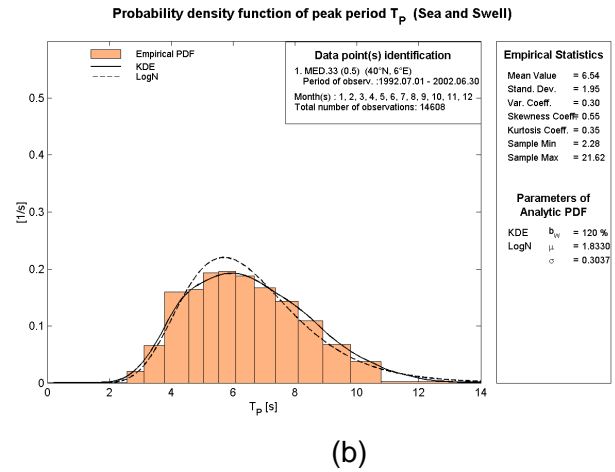
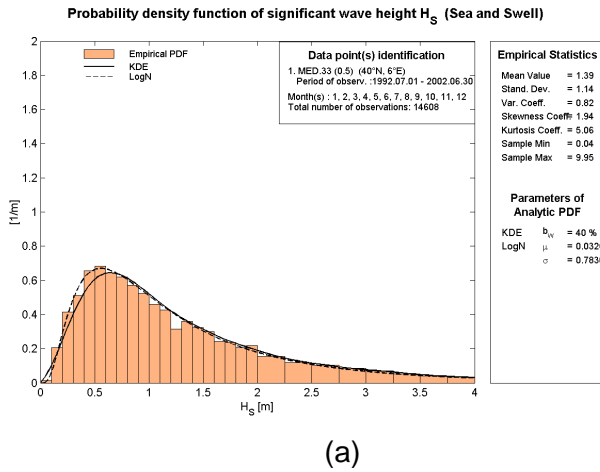


Figure 13 - Examples of univariate wave statistics for datapoint (6E,40N).
(a) Significant wave height, (b) Peak period, (c) Wave slope, (d) Wave direction.

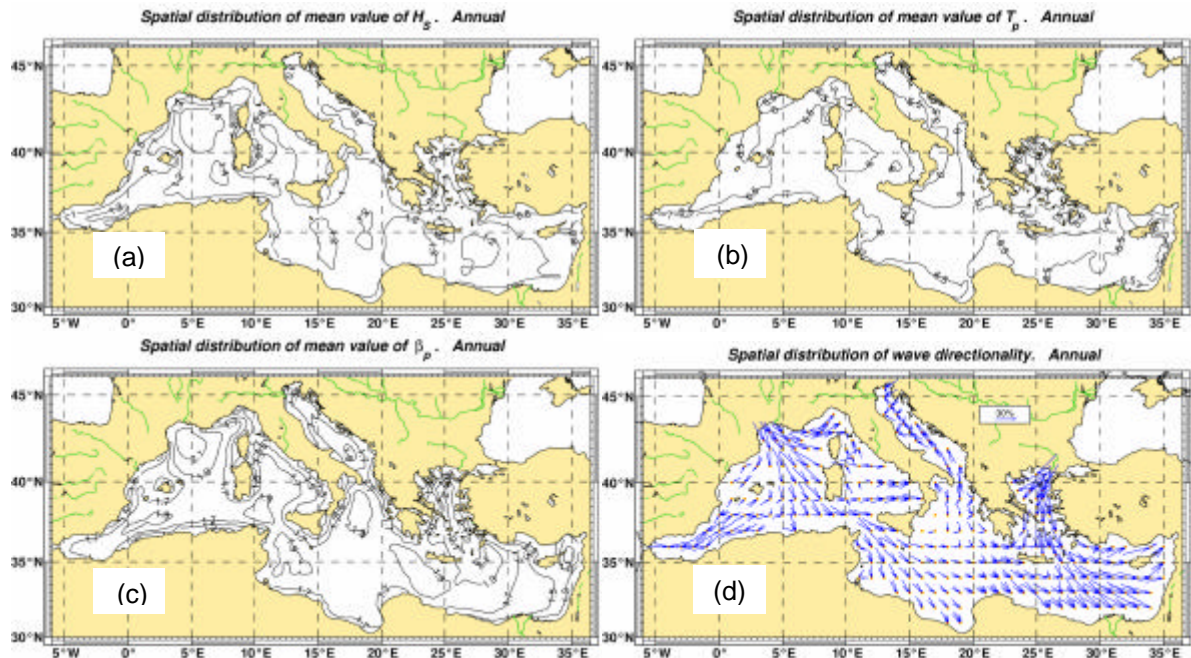


Figure 14 - Examples of spatial wave statistics.
(a) Significant wave height, (b) Peak period, (c) Wave slope, (d) Wave direction.

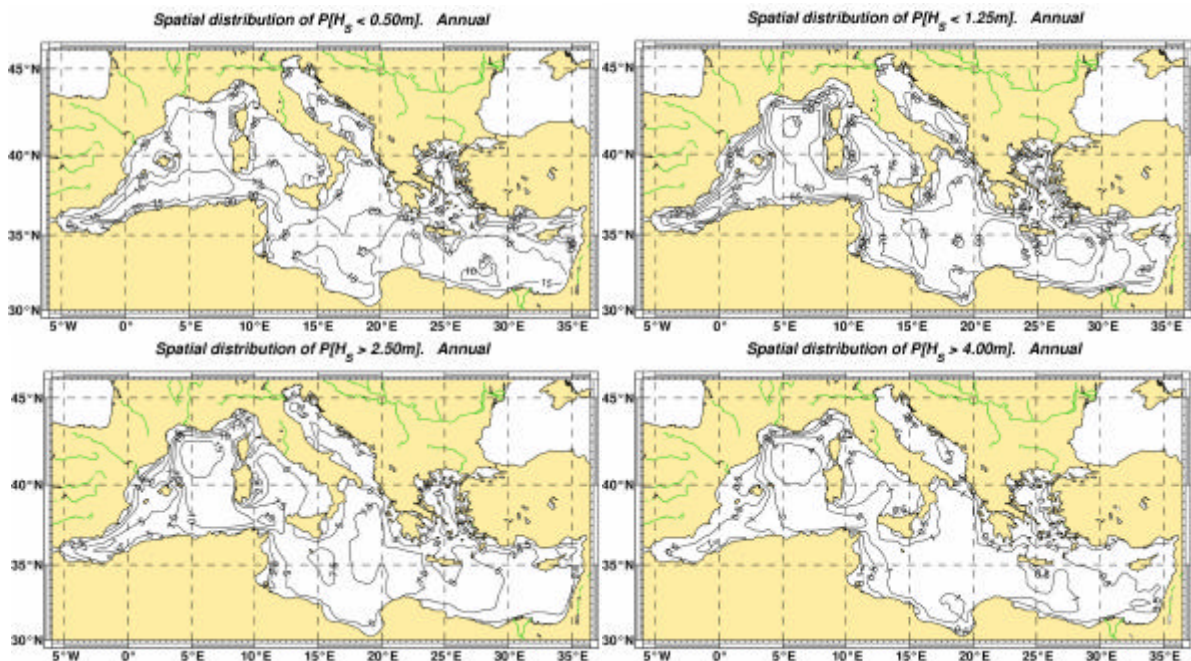


Figure 15 - Examples of spatial distribution of some important wave events

5.5.3. Joint statistics

The following joint wind-wave parameters have been considered:

- Significant wave height and Wind speed
(H_s, U_w)

In Figure 16, the joint empirical pdf of H_s and U_w is given for a specific datapoint (site) in the Western Mediterranean Sea. It is shown that this pdf is well approximated by the KDM representation. The joint empirical probability density function, given for 129 points throughout the Mediterranean Sea, provides us with valuable information about the correlation of wind speed and significant wave height.

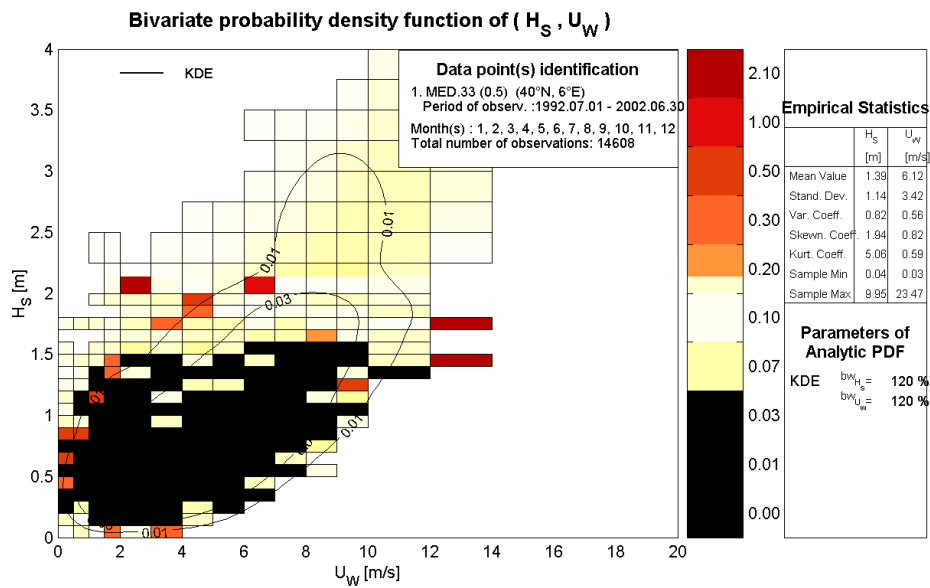


Figure 16 - Joint wind-wave statistics for datapoint (6E,40N)

6. Reliability assessment of the atlas

6.1. Critical analysis of the reliability of the calibrated data

In section 4.4, we have analysed the single steps of the calibration procedure and pointed out the single sources of error. The seemingly random errors present in the results of any numerical model are partly compensated during the statistical analysis. However, most of the error sources discussed in 4.4 are numerical and instrumental, with often a permanent bias of the data. In principle a bias can be taken into account by the calibration. This is what a calibration is about. Unluckily this is not the case when the errors are not constant during the considered period, and each sub-period, during which the modelling and measurement conditions are kept constant, is not long enough to allow a separate calibration.

Other errors are known in principle, but the correction is not possible. This is the case for the underestimate of the wave conditions in the early stages of generation, present for many years in the WAM model. Because the single wave height values at a given time can be the result of wind-wave interaction for many hours before the time we are considering, it is not possible to know on a systematic basis the stage of generation along the whole time series. So no correction is possible.

Other sources of error are known in principle, but not enough to be able to formulate an algorithm to correct the data. This is the case of the wind speed derived from altimeters and scatterometers. The retrieved values are strongly dependent on the sea state, in particular if the waves are, e.g., locally generated, well developed or a far coming swell. The algorithms presently used to transform the return signal into wind speed have been calibrated with extensive campaigns in the open oceans, where the wave conditions are substantially different from those present in the enclosed seas, like the Mediterranean. We are sure this has consequences, but not enough data exist to suggest the proper modification of the algorithms in the enclosed seas.

An obvious source of error is the presence of the coast. Its description with a finite grid is always approximate. Except the case when the waves move perpendicularly towards the coast, its approximate geometry is likely to affect the local results. This is more evident when the coastline is complicated, with protruding peninsulas, bays, islands, etc. Unluckily this is the case for large part of the Mediterranean coastline, especially in its northern side. The problem is more manifest in the smaller basins or around small islands, poorly defined from the geometrical point of view. It becomes critical in areas characterised by clusters of islands. The obvious example is the Aegean Sea, where only a fraction of the islands is present, with a resolution of about 25 km, in the grid.

6.2. Geographical distribution of the reliability

Summarising the discussion in sections 4.4 and 6.1, the main sources of error are:

- 1) seemingly random errors in the model results,
- 2) the poor performance and the lack of data from satellites in the coastal areas, more extended when flying offshore,
- 3) the underestimate of the wave conditions in the early stages of generation. This was present in the WAM model till December 1996,
- 4) the continuous upgrading of the meteorological and wave models, with a consequent variation of performance. Only the main one, the passage to T511 in November 2000, has been taken into account,
- 5) the period considered for T511, from November 2000 till June 2002, is too short for a reliable calibration,
- 6) the wind speeds from the altimeters have an error whose quantity is unknown. Obviously this is reflected in the calibrated data.
- 7) the approximate geometry of the coast and the poor representation of small islands in the computational grid.

The consequent geographical distribution of the errors is partly represented in Figure 6 and Figure 7. The larger the scatter index, the larger the uncertainty of the results. So we see that the quality of the results improve while moving from north to south in the basin. The worst results are found along the European coast, particularly in enclosed areas, like the Ligurian Sea, the Adriatic Sea, the Aegean Sea, and the coast of Turkey.

In general the results are not reliable close to the coasts, the more so the more complicated the geometry of the coastline. This makes the results around islands quite doubtful, particularly when their dimensions are of the same order of magnitude of the resolution of the grid (20-28 km). The worst areas in this respect are the East coast of the Adriatic Sea and the Aegean Sea. With over 1000 islands and only a tiny fraction of them represented in the computational grid, the latter one is the extended area with the more doubtful results.

7. Printed Atlas

The Printed atlas is divided in two parts: Part A and Part B. The Part A contains background material and a short description of the data. The second part (Part B) contains the statistical results presented either in graphical form (70 charts on maps) or in tabular form (2580 bivariate histograms).

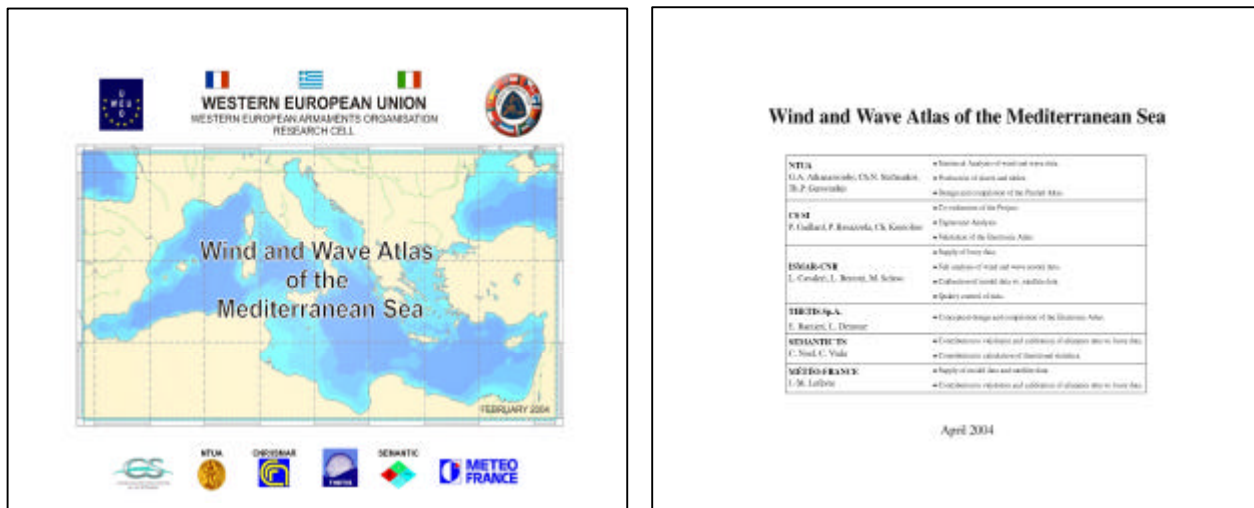


Figure 17 - The cover and the first page of the atlas

In Part A, a brief theoretical background is presented. The wind and wave parameters considered are defined and the corresponding wind and wave data (time series used for statistical analysis) are described. Moreover, details concerning the calibration of the model data using satellite ones are given, including information about the reliability of the calibrated data. Then, a description of the statistical analysis follows, including models used, results obtained etc.

Part B contains three categories of statistical results:

- Category 1: Spatial distribution of statistical quantities
- Category 2: Spatial distribution of probabilities of some important events
- Category 3: Frequency tables of joint occurrences

The first two categories are in graphic format (they contain maps and charts), while the third one contains tables.

Information content for all categories is considered on a seasonal basis. The following season definition has been used:

- a. Autumn: *September, October, November*
- b. Winter: *December, January, February*
- c. Spring: *March, April, May*
- d. Summer: *June, July, August*
- e. Annual: *All months*

7.1. Spatial distribution of statistical quantities

The first category includes the following items:

1. Charts of mean wind speed
2. Charts of wind direction
3. Charts of mean wave height
4. Charts of mean period
5. Charts of mean wave slope
6. Charts of wave direction

The maps in No. 1., 3., 4., 5., present contour lines of mean values of the wind and wave parameters are depicted. Contours are the locus of sites where the (seasonal) mean value is constant. This constant value is depicted on each contour.

In the maps No. 2., 6., arrows show the direction from which wind blows or wave comes (FROM definition). The length of the arrows corresponds to the frequency of occurrence (%) of winds/waves coming from the corresponding direction. Directions with frequency of occurrence less than 10% are not drawn. Twenty four (24) directions are considered: 0 (N), 15, 30, 45 (NE), 60, 75, 90 (E), 105, 120, 135 (SE), 150, 165, 180 (S), 195, 210, 225 (SW), 240, 255, 270 (W), 285, 300, 315 (NW), 330, 345.

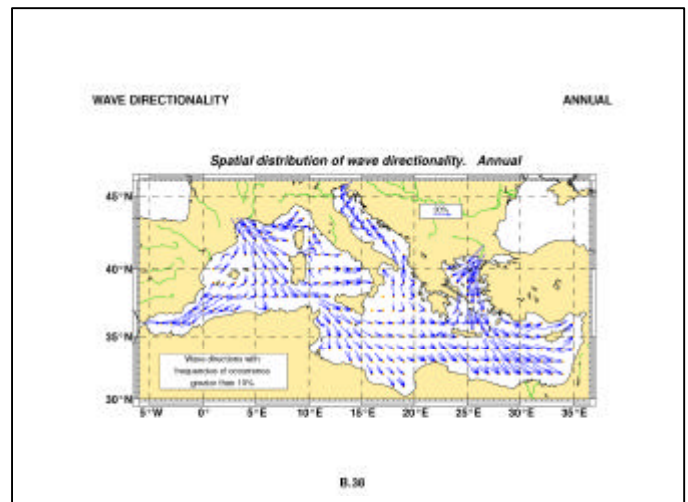
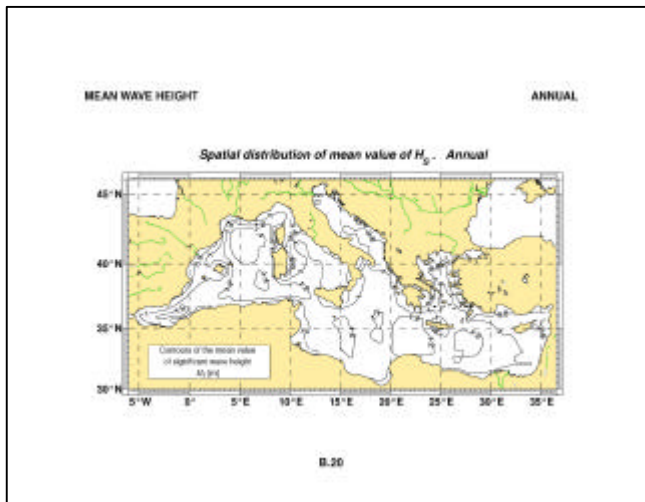
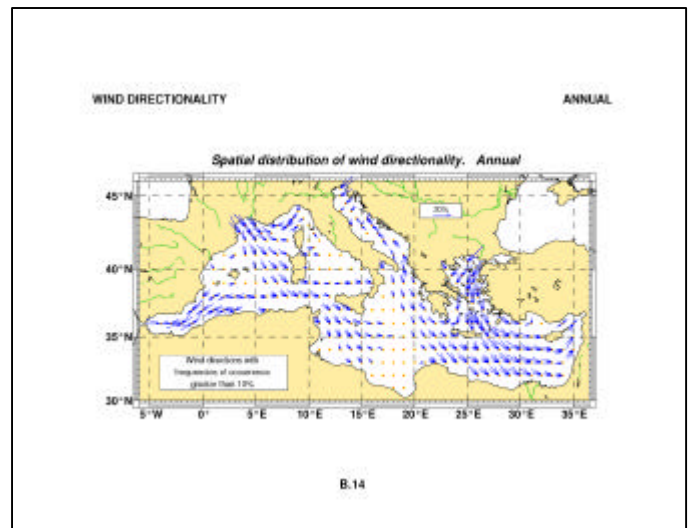
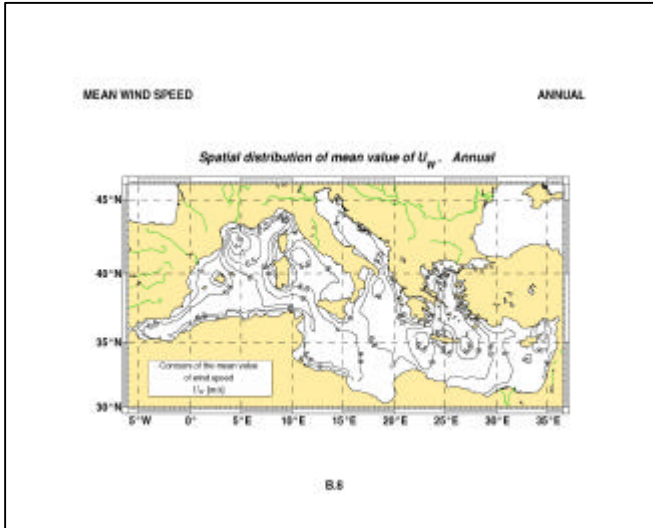


Figure 18 - Sample pages of the first category

7.2. Spatial distribution of probabilities of some important events

The second category includes the following items:

1. Charts of wind speed isopleths
 - a. $P[U_W < 4m/s]$
 - b. $P[U_W < 6m/s]$
 - c. $P[U_W > 8m/s]$
 - d. $P[U_W > 11m/s]$
2. Charts of wave height isopleths
 - a. $P[H_S < 0.5m]$
 - b. $P[H_S < 1.25m]$
 - c. $P[H_S > 2.5m]$
 - d. $P[H_S > 4m]$

Wind speed/ Wave height isopleths are the locus of sites where the frequency of occurrence of the events $[U_W < U_{W,threshold}]$, $[U_W > U_{W,threshold}]$, $[H_S < H_{S,threshold}]$ or $[H_S > H_{S,threshold}]$ has a constant value. This constant value (in %) is depicted on each isopleth.

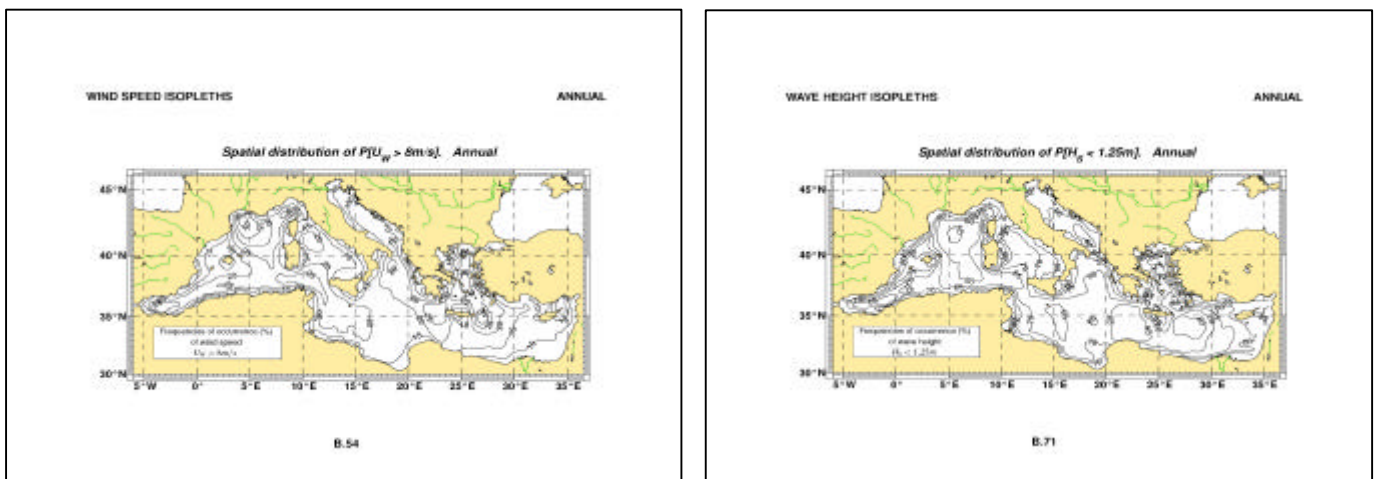


Figure 19 - Sample pages of the second category

7.3. Frequency tables of joint occurrences

The third category includes the following items:

1. Histograms of wind speed-wind direction
2. Histograms of wave height-wave period
3. Histograms of wave height-wave direction
4. Histograms of wave height-wind speed

Histograms are given for 129 datapoints in the Mediterranean Sea. Each entry of the joint (two-dimensional) histogram denotes the number of observations per thousand associated with the corresponding cell of the bivariate partition of the corresponding parameters. Marginal (one-dimensional) histograms of wind and wave parameters are also given.

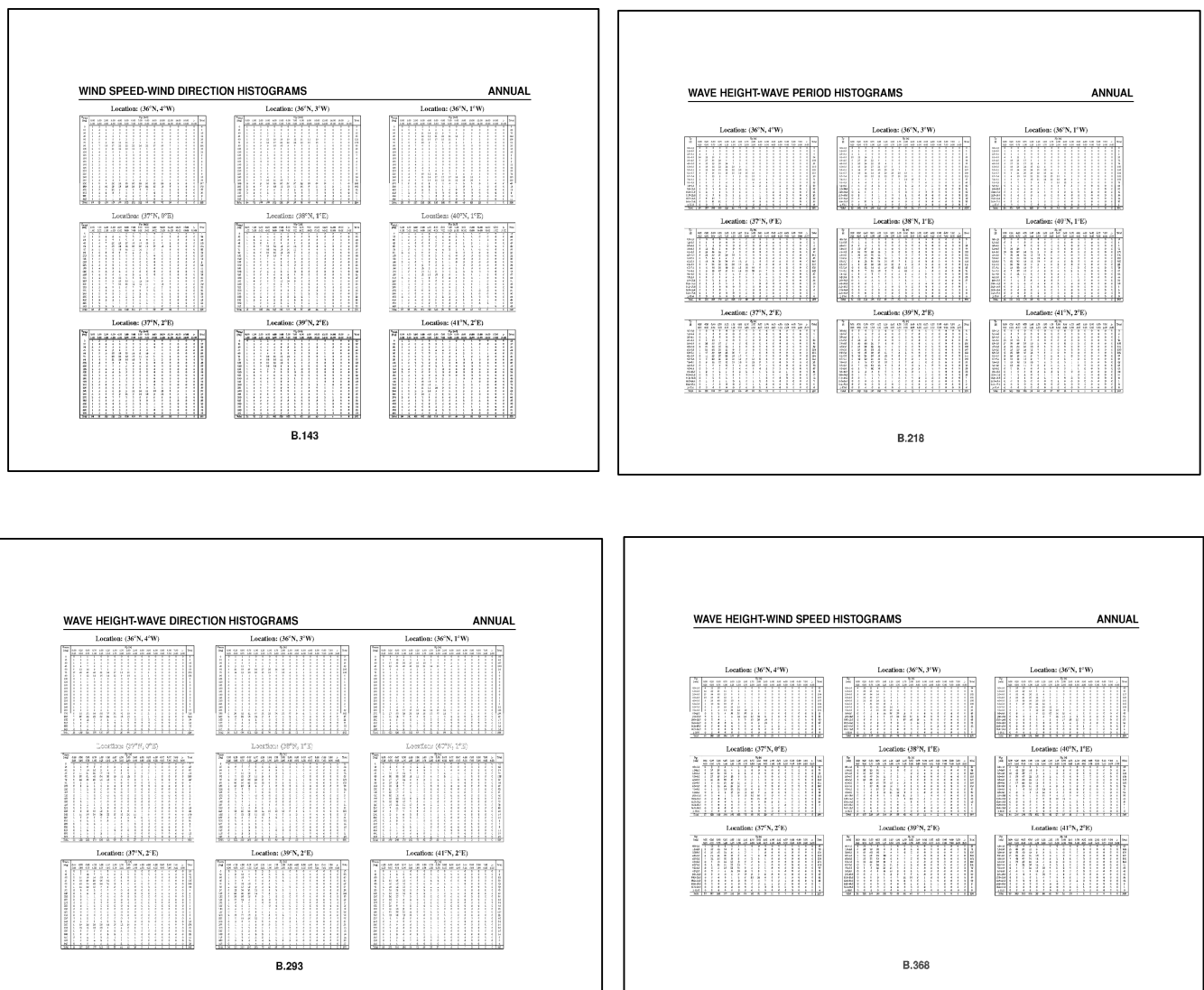


Figure 20 - Sample pages of the third category

8. References

Aivazian, S., Enukov, I., Mechalkine, L., 1986, *Elements de modelisation et traitement primaire des donnees*, MIR Publishers, Moscow.

Andrew, R.N. and W.G. Price, 1978, Applications of generalized gamma functions in ship dynamics, *Trans. Royal Inst. Naval Architects (RINA)*, 1978, pp. 137-143.

Athanassoulis, G.A. and Ch.N. Stefanakos, 1995, A nonstationary stochastic model for long-term time series of significant wave height, *Journal of Geophysical Research*, Vol. 100, No. C8, pp. 16149-16162.

Athanassoulis G.A. and Ch.N. Stefanakos, 1996a, "Statistical analysis of wave data. Ia: Univariate statistics/Mediterranean Sea", NTUA Report, WERATLAS Project, JOU2-CT93-0390, 35+85+85pp.

Athanassoulis, G.A. and Ch.N. Stefanakos, 1996b, Statistical Analysis of wave data. IIa: Bivariate statistics/Mediterranean Sea, NTUA Report, WERATLAS Project, JOU2-CT93-0390, April 1996.

Athanassoulis, G.A. and Ch.N. Stefanakos, 1996c, Statistical analysis of wave data. IIIa: Directional statistics/Mediterranean Sea. Part 1: Theoretical background, Greek contribution to WERATLAS project, JOU2-CT93-0390, May 1996.

Athanassoulis, G.A. and Ch.N. Stefanakos, 1998, Missing-value completion of nonstationary time series of wave data, 17th International Conference on Offshore Mechanics and Arctic Engineering, Lisbon, Portugal, July 5-9, 1998.

Athanassoulis G.A., Stefanakos, Ch.N., 2001, "Time Series Statistics", Greek contribution to MEDATLAS project, Contract No. 99/RFP10.10/009, July 2001 (70pp.).

Athanassoulis, G.A. and K.A. Belibassakis, 1999, Analytic representation of multivariate distributions by means of kernel density models with application to ocean wave data, EUROWAVES project report no. SCR/18, MAS3-CT97-0109, July 1999.

Athanassoulis, G.A. Belibassakis, K.A., 2002, "Probabilistic description of metocean parameters by means of kernel density models. 1. Theoretical background and first results", *Applied Ocean Research*, Vol. 24, pp. 1-20.

Athanassoulis, G.A. E.K. Skarsoulis and K.A. Belibassakis, 1994, Bivariate distributions with given marginals with an application to wave climate description, *Applied Ocean Research*, Vol. 16, No. 1, pp. 1-17.

Athanassoulis, G.A. E.K. Skarsoulis, 1992, *Wind and Wave Atlas of the North-Eastern Mediterranean Sea*, Ship and Marine Hydrodynamics Laboratory, National Technical University of Athens.

Athanassoulis, G.A., Vranas, P. and T.S. Soukissian, 1992, A new model for long-term stochastic analysis and prediction--Part I: Theoretical background, *Journal of Ship Research*, Vol. 36, No. 1, pp. 1-16.

Barstow, S.F., G.A. Athanassoulis, L. Cavaleri, G. Mork, K.A. Belibassakis, Ch.N. Stefanakos, Th.P. Gerostathis, M. Sclavo, L. Bertotti, and H.E. Krogstad, 2001, EUROWAVES: A user-friendly tool for the evaluation of wave conditions at any European coastal location, Mast3 Project CT97-0109, Final technical Report.

Belberova, D., and D. Myrhaug, 1996, Critical assessment of the joint occurrence of wind and waves at a buoy station off the southern Norwegian coast, *Journal of Wind Engineering and Industrial Aerodynamics*, Vol. 61, 207-224.

Bidlot, J.R., D.H.Holmes, P.A.Wittmann, R.Lalbeharry, and H.S.Chen, 2001, "Intercomparison of the performance of operational ocean wave forecasting systems with buoy data", ECMWF, Tech.Memo 315, 46pp.

Bitner-Gregersen, E.M. and E.H. Cramer, 1995, Uncertainties of load characteristics and fatigue damage of ship structures, *Marine Structures*, 1995, No. 8, pp. 97-117.

Bitner-Gregersen, E.M., C. Guedes Soares and A. Silvestre, 1998, On the average wave steepness, *Ocean Wave Kinematics, Dynamics and Loads on Structures, Proc. of the 1998 International OTRC Symposium*, April 30 -May 1, 1998, pp. 513-520, Houston, Texas.

Bitner-Gregersen, E.M., C.G. Soares, U. Machado and P. Cavaco, 1998, Comparison of different approaches to joint environmental modelling, *Proceedings of the 17th International Conference on Offshore Mechanics and Arctic Engineering*, OMAE, Lisbon, Portugal, 5-9 July, 1998

Cavaleri, L., and L.Bertotti, 2003a, The characteristics of wind and wave fields modelled with different resolutions, *Q.J.R.Meteorol.Soc.*, **129**, pp.1647-1662.

Cavaleri, L., and L.Bertotti, 2003b, The accuracy of modelled wind and wave fields in enclosed seas, in publication on *Tellus*.

Cavaleri, L., Bertotti, L., Sclavo, M., 2000, Comparison between model and buoy measured wave parameters, ISDGM Report, 2000.

Cavaleri, L., Bertotti, L., Sclavo, M., Ramieri, E., 2002, Calibration of wind and wave model data in the Mediterranean Sea – The extended period July 1992 – June 2002, ISDGM Report, 2002.

Cavaleri, L., L.Bertotti, and P.Lionello, 1991, Wind wave cast in the Mediterranean Sea, *J.Geophys.Res.*, **96**, No.C6, pp.10,739-10,764.

Challenor, P. G., and O. D. Cotton, (1997)., The SOC contribution to the ESA working group calibration and validation of ERS-2 FD measurements of significant wave height and wind speed. In "Proceedings CEOS Wind and wave validation workshop", pp. 81-93, 3-5 June, 1997, ESTEC , Noordwijk, The Netherlands

Chen, S.X., 1999, Beta kernel estimators for density functions, *Computational Statistics and Data Analysis*, Vol. 31, pp. 131-145.

Cotton, P. D., Challenor, P. G., and D. J. T. Carter (1997). An assessment of the accuracy and reliability of Geosat, ERS-1, ERS-2, and TOPEX altimeter measurements of significant wave height and wind speed. In "Proceedings CEOS Wind and wave validation workshop", pp. 81-93, 3-5 June, 1997, ESTEC , Noordwijk, The Netherlands.

Dacunha, N.M.C., M. Hogben and K.S. Andrews, 1984, Wave climate synthesis worldwide, *Proc. of International Symposium on Wave and Wind Climatology Worldwide*, The Royal Inst. of Naval Architects (RINA), 1984, London.

De Boni, M., L.Cavaleri, and A.Rusconi, 1993, "The Italian wave measurement network", *23^d Int.Conf.Coast.Eng.*, pp.116-128, 4-9 October 1992, Venice, 3520pp.

Dell'Osso, L., L.Bertotti,, and L.Cavaleri, 1992, The GORBUSH storm in the Mediterranean Sea: atmospheric and wave simulation, *Monthly Weather Review*, **120**, No.1, pp.77-90.

Direccion General de Puertos y Costas, 1988, *Atlas Basado sobre Observaciones Visuales de Barcos en Ruta*.

ERS user handbook ESA SP 11-48.

Fang, Z., Dai Shunsun and Jin Chengyi, 1989, On the long-term joint distribution of characteristic wave height and period and its application, *Acta Oceanologica Sinica*, Vol. 8, No. 3, pp. 315-325.

Fang, Z.S. and N. Hogben, 1982, *Analysis and Prediction of Long-term Probability Distributions of Wave Heights and Periods*, Report, National Maritime Institute, 1982, London.

Feld, G. and J. Wolfram, 1996, Bivariate modelling of H and T , *15th International Offshore Mechanics and Arctic Engineering Conference*, 1996, Vol. 2, Florence, Italy.

Ferreira, J.A. and C. Guedes Soares, 1999, Modelling the long-term distribution of significant wave height with the Beta and Gamma models, *Ocean Engineering*, Vol. 26, pp. 713-725.

Fisher, N.I. 1993, *Statistical Analysis of Circular Data*, Cambridge University Press, Cambridge, 1993.

Fix, E. and Hodges, J.L., 1951, Nonparametric discrimination: Consistency properties, Rep. No4, USAF School of Aviation Medicine, Randolph Field, Texas.

Goda, Y. 2000, *Random seas and design of maritime structures*, World Scientific.

Gran, S., 1992, *A Course in Ocean Engineering*, Elsevier Science Publishers, Amsterdam.

Hardle, W., 1991, *Smoothing techniques with implementation in S*, Springer Verlag.

Haver, S., 1985, Wave climate off northern Norway", *Applied Ocean Research*, Vol. 7, 85-92.

Hogben, N., 1990, Long term wave statistics, *The Sea*, (Le Mahaute, B. and D.M. Hanes, eds.), J. Wiley & Sons, New York, Vol. 9A, 293-333.

Hogben, N., Dacunha and Ollivier, 1986, *Global Wave Statistics*.

IAHR working group, 1989, List of sea-state parameters, *Journal of Waterway, Port, Coastal, and Ocean Engineering*, Vol. 115, No. 6, pp. 793-808, 1989.

Ivchenko, G., Medvedev, Yu., 1990, *Mathematical statistics*, MIR Publishers, Moscow.

Janssen, P.A.E.M., 1998, On error growth in wave models, Tech.Memo. No.249, ECMWF, 12pp.

Jasper, N.H., 1956, Statistical distribution patterns of ocean waves and of wave-induced ship stresses and motions with engineering applications", *Transactions of The Society of Naval Architects and Marine Engineers*, 1956, Vol. 64, pp. 375-432.

Johnson, N., Kotz, S., 1970, *Continuous univariate distributions*, Houghton Mifflin Co., Boston.

Komen, G.J., L.Cavaleri, M.Donelan, K.Hasselmann, S.Hasselmann, and P.A.E.M.Janssen, 1994, *Dynamics and Modelling of Ocean Waves*, Cambridge University Press, 536pp.

Krogstad, H.E., 1985, Height and period distributions of extreme waves, *Applied Ocean Research*, Vol. 7, No. 3, pp. 158-165.

Lefevre J.-M. and Cotton D., (2001). " Ocean Surface Waves", in Fu, L.L., and Cazenave, A., editors,

Satellite Altimetry and Earth Sciences", *Academic Press*, International Geophysics Series, Vol 69, 463p.

Longuet-Higgins, M.S, Cartwright, D.E. and N.D. Smith, 1963, Observations of the directional spectrum of sea waves using the motion of a floating buoy in: *Ocean Wave Spectra*, Prentice-Hall, pp. 111-136.

Longuet-Higgins, M.S., 1957, The statistical analysis of a random, moving surface, *Philosophical Transactions of the Royal Society of London, Series A*, Vol. 249, pp. 321-387.

Mardia, K.V., 1972, *Statistics of directional data*, Academic Press.

Mathiesen, J. and E. Bitner-Gregersen, E., 1990, Joint distributions for significant wave height and wave zero-upcrossing period, *Applied Ocean Research*, 1990, Vol. 12, pp. 93-103.

Moerk G. and S.F. Barstow, 1998a, Comparison of WAM estimates of H_s with TOPEX/POSEIDON altimeter data in the Mediterranean Sea; a comparison of low and high resolution wind models, EUROWAVES project report no.SCR/1 MAS3-CT97-0109, July 1998.

Moerk G. and S.F. Barstow, 1998b, Comparison of WAM estimates of H_s with TOPEX/POSEIDON altimeter data in European Atlantic waters; a comparison of low and high resolution wind models, EUROWAVES project report no.SCR/2, MAS3-CT97-0109, September 1998.

Moerk G. and S.F. Barstow, 1999, Comparison of WAM estimates of H_s with TOPEX altimeter data in the Baltic and Black Sea, EUROWAVES project report no. SCR/31, MAS3-CT97-0109, March 1999.

Monbet, V., M. Prevosto and J. Deshayes, 1995, Approximation of up crossing of high level for the acceleration of the response of a non linear stochastic oscillator, *7th International Conference of Applications of Statistics and Probability*, Paris.

Naval Oceanography Command Detachment, 1983, U.S. Navy Hindcast Spectral Ocean Wave Model Climatic Atlas: North-Atlantic Ocean.

Nordenstrom, N., 1969, Methods for predicting long-term distributions of wave loads and probability of failure for ships. Part I: Environmental conditions and short term response, Report 69-21-S, Det Norske Veritas.

Ochi, M.K. 1998 *Ocean waves. The stochastic approach*, Cambridge University Press

Ochi, M.K., 1978, Wave statistics for the design of ships and ocean structures, *Transactions of The Society of Naval Architects and Marine Engineers*, 1978, Vol. 60, pp. 47-76.

Ochi, M.K., 1982, Stochastic analysis and probabilistic prediction of random seas, *Advances in Hydroscience*, Vol. 13, pp. 217-375, 1982.

Parzen, E., 1962, On estimation of a probability density function and mode", *The Annals of Mathematical Statistics*, Vol. 33, No. 3, pp. 1065-1076.

Philips, O.M., 1977, *The dynamics of the upper ocean*, Cambridge University Press (2nd edition).

Plackett, R.L., 1965, A class of bivariate distributions. *J. Am. Statist. Assoc.*, Vol. 60, 516-522.

Queffeuou P, 1996, Significant wave height and backscatter coefficient at ERS1/2 and TOPEX-POSEIDON ground-track crossing points FDP, Final report, ESA contract 143189, Department d'Océanographie Spatial, IFREMER.

Queffeuou P., A. Bentamy, Y. Quilfen and J. Tournadre, Validation of ERS-1 and TOPEX-POSEIDON



**METEO
FRANCE**

Scientific Report RTP10.10

altimeter wind and wave measurements, Document de travail DRO-OS 94-08, Ifremer, Decembre 1994.

Scott, D.W., 1992, *Multivariate density estimation. Theory, Practice and Visualisation*, John Wiley & Sons.

Silverman, B.W., 1986, *Density estimation*, Chapman and Hall.

Simmons, A., 1991: Development of the operational 31-level T213 version of the ECMWF forecast model, *ECMWF Newsletter*, **56**, pp.3-13.

Simmons, A., R.Mureau, and T.Petroligis, 1995: Error growth and predictability estimates for the ECMWF forecasting system, *Q.J.Roy.Meteor.Soc.*, **121**, pp.1739-1771.

Simonoff, J.S., 1996, *Smoothing methods in statistics*, Springer-Verlag.

Soares, Guedes C., L.C. Lopes and M.D.S. Costa, 1988, Wave climate modelling for engineering purposes, Proceedings of an International Conference on Computer Modelling in Ocean Engineering, B.A. Schrefler and O.C. Zienkiewicz (eds.), Venice, Italy, 19-23 September 1988, pp. 169-175.

Stefanakos, Ch.N., 1999, Nonstationary stochastic modelling of time series with applications to environmental data, Ph.D. Thesis, National Technical University of Athens, Dept. of Naval Architecture and Marine Engineering, Athens, Greece.

Swail, V.R., and A.T.Cox, 2000, On the use of NCEP-NCAR reanalysis surface marine wind fields for a long-term North Atlantic wave hindcast, *J.of Atmsph. And Ocean. Tech.*, Vol.17, pp.532-545.

WAM-DI Group, 1988, The WAM model – a third generation ocean wave prediction model, *J.Physic.Oceanog.*, **18**, pp.1775-1810.

Wand, M.P., Jones, M.C., 1995, *Kernel smoothing*, Chapman & Hall.